



THE UNIVERSITY *of* EDINBURGH

Edinburgh Research Explorer

De novo assembly of a 40 Mb eukaryotic genome from short sequence reads

Citation for published version:

Nowrousian, M, Stajich, JE, Chu, M, Engh, I, Espagne, E, Halliday, K, Kamerewerd, J, Kempken, F, Knab, B, Kuo, H-C, Osiewacz, HD, Pöggeler, S, Read, ND, Seiler, S, Smith, KM, Zickler, D, Kück, U & Freitag, M 2010, 'De novo assembly of a 40 Mb eukaryotic genome from short sequence reads: *Sordaria macrospora*, a model organism for fungal morphogenesis', *PLoS Genetics*, vol. 6, no. 4, e1000891. <https://doi.org/10.1371/journal.pgen.1000891>

Digital Object Identifier (DOI):

[10.1371/journal.pgen.1000891](https://doi.org/10.1371/journal.pgen.1000891)

Link:

[Link to publication record in Edinburgh Research Explorer](#)

Document Version:

Publisher's PDF, also known as Version of record

Published In:

PLoS Genetics

Publisher Rights Statement:

This is an open-access article distributed under the terms of the Creative Commons Attribution License, which permits unrestricted use, distribution, and reproduction in any medium, provided the original author and source are credited.

General rights

Copyright for the publications made accessible via the Edinburgh Research Explorer is retained by the author(s) and / or other copyright owners and it is a condition of accessing these publications that users recognise and abide by the legal requirements associated with these rights.

Take down policy

The University of Edinburgh has made every reasonable effort to ensure that Edinburgh Research Explorer content complies with UK legislation. If you believe that the public display of this file breaches copyright please contact openaccess@ed.ac.uk providing details, and we will remove access to the work immediately and investigate your claim.



De novo Assembly of a 40 Mb Eukaryotic Genome from Short Sequence Reads: *Sordaria macrospora*, a Model Organism for Fungal Morphogenesis

Minou Nowrousian¹, Jason E. Stajich², Meiling Chu³, Ines Engh¹, Eric Espagne⁴, Karen Halliday⁵, Jens Kamerewerd¹, Frank Kempken⁶, Birgit Knab⁷, Hsiao-Che Kuo^{3*}, Heinz D. Osiewacz⁷, Stefanie Pöggeler⁸, Nick D. Read³, Stephan Seiler⁹, Kristina M. Smith¹⁰, Denise Zickler⁴, Ulrich Kück^{1*}, Michael Freitag^{10*}

1 Lehrstuhl für Allgemeine und Molekulare Botanik, Ruhr-Universität Bochum, Bochum, Germany, **2** Department of Plant Pathology and Microbiology, University of California Riverside, Riverside, California, United States of America, **3** Fungal Cell Biology Group, Institute of Cell Biology, University of Edinburgh, Edinburgh, United Kingdom, **4** Institut de Génétique et Microbiologie, Université Paris Sud, Orsay, France, **5** Institute of Molecular Plant Sciences, Biological Sciences, University of Edinburgh, Edinburgh, United Kingdom, **6** Abteilung Botanische Genetik und Molekularbiologie, Botanisches Institut und Botanischer Garten, Christian-Albrechts-Universität zu Kiel, Kiel, Germany, **7** Institute of Molecular Biosciences, Faculty for Biosciences and Cluster of Excellence Macromolecular Complexes, Johann Wolfgang Goethe University, Frankfurt, Germany, **8** Institute of Microbiology and Genetics, Department of Genetics of Eukaryotic Microorganisms, Georg-August University, Göttingen, Germany, **9** Institute of Microbiology and Genetics, Department of Molecular Microbiology and Genetics, DFG Research Center Molecular Physiology of the Brain (CMPB), Georg-August University, Göttingen, Germany, **10** Center for Genome Research and Biocomputing, Department of Biochemistry and Biophysics, Oregon State University, Corvallis, Oregon, United States of America

Abstract

Filamentous fungi are of great importance in ecology, agriculture, medicine, and biotechnology. Thus, it is not surprising that genomes for more than 100 filamentous fungi have been sequenced, most of them by Sanger sequencing. While next-generation sequencing techniques have revolutionized genome resequencing, e.g. for strain comparisons, genetic mapping, or transcriptome and ChIP analyses, *de novo* assembly of eukaryotic genomes still presents significant hurdles, because of their large size and stretches of repetitive sequences. Filamentous fungi contain few repetitive regions in their 30–90 Mb genomes and thus are suitable candidates to test *de novo* genome assembly from short sequence reads. Here, we present a high-quality draft sequence of the *Sordaria macrospora* genome that was obtained by a combination of Illumina/Solexa and Roche/454 sequencing. Paired-end Solexa sequencing of genomic DNA to 85-fold coverage and an additional 10-fold coverage by single-end 454 sequencing resulted in ~4 Gb of DNA sequence. Reads were assembled to a 40 Mb draft version (N50 of 117 kb) with the Velvet assembler. Comparative analysis with *Neurospora* genomes increased the N50 to 498 kb. The *S. macrospora* genome contains even fewer repeat regions than its closest sequenced relative, *Neurospora crassa*. Comparison with genomes of other fungi showed that *S. macrospora*, a model organism for morphogenesis and meiosis, harbors duplications of several genes involved in self/nonself-recognition. Furthermore, *S. macrospora* contains more polyketide biosynthesis genes than *N. crassa*. Phylogenetic analyses suggest that some of these genes may have been acquired by horizontal gene transfer from a distantly related ascomycete group. Our study shows that, for typical filamentous fungi, *de novo* assembly of genomes from short sequence reads alone is feasible, that a mixture of Solexa and 454 sequencing substantially improves the assembly, and that the resulting data can be used for comparative studies to address basic questions of fungal biology.

Citation: Nowrousian M, Stajich JE, Chu M, Engh I, Espagne E, et al. (2010) *De novo* Assembly of a 40 Mb Eukaryotic Genome from Short Sequence Reads: *Sordaria macrospora*, a Model Organism for Fungal Morphogenesis. PLoS Genet 6(4): e1000891. doi:10.1371/journal.pgen.1000891

Editor: Paul M. Richardson, Progentech, United States of America

Received: December 24, 2009; **Accepted:** March 2, 2010; **Published:** April 8, 2010

Copyright: © 2010 Nowrousian et al. This is an open-access article distributed under the terms of the Creative Commons Attribution License, which permits unrestricted use, distribution, and reproduction in any medium, provided the original author and source are credited.

Funding: Solexa sequencing was supported by start-up funds from the OSU Computational and Genome Biology Initiative and Oregon State University to MF. MN and UK were supported by grants from the German Science foundation (DFG, Deutsche Forschungsgemeinschaft, NO 407/2-1 and SFB480) and the Protein Research Department (PRD, Ruhr-Universität Bochum). SP was supported by the German Science Foundation (DFG, Deutsche Forschungsgemeinschaft, PO523/3-2). SS was supported through the DFG Research Center of Molecular Physiology of the Brain (CMPB) and the DFG Priority Program Cell Polarity (SP1111). KMS was supported by a grant from the American Cancer Society (RSG-08-030-01-CCG to MF). NDR and KH were funded by the Biotechnological and Biological Sciences Research Council (grant no. BB/F013574). The funders had no role in study design, data collection and analysis, decision to publish, or preparation of the manuscript.

Competing Interests: The authors have declared that no competing interests exist.

* E-mail: ulrich.kueck@rub.de (UK); freitagm@cgrb.oregonstate.edu (MF)

† Current address: Institute of Biotechnology, National Cheng Kung University, Tainan, Taiwan

Introduction

Fungi are heterotrophic eukaryotes found in nearly all ecosystems. About 100,000 fungi have been described to date, but conservative estimates predict at least 1.5 million different

species [1,2]. Fungi exhibit a wide range of different lifestyles, particularly as saprobes, pathogens or symbionts. As saprobes, fungi acquire nutrients from dead organic matter and are among the main recyclers on the planet. They play important roles in the degradation of cellulose and lignin, contributing greatly to the

Author Summary

Fungi have immense impacts on ecosystems and affect many aspects of society. They are used as convenient organisms for fundamental research because their typically haploid genetics enable straightforward phenotyping of mutations and because most fungal cells can differentiate the entire organism. Fungi have compact genomes with few repetitive sequences, and their genomes should be much easier to assemble from short sequence reads than genomes of mammals or higher plants. To test this idea, we used Solexa and 454 sequencing to generate ~4 Gb of raw sequence data from the filamentous fungus *Sordaria macrospora*. *De novo* assembly yielded 5,097 contigs. This assembly was improved by comparison with reference genomes of three closely related *Neurospora* species, resulting in placement of ~40 Mb of genome sequence in 152 scaffolds. From comparisons of predicted proteins we conclude that *S. macrospora* carries a conserved set of genes for signaling and development, which should encourage its further use as a model organism for morphogenesis and meiosis. We demonstrate that *de novo* assembly of fungal genomes from short reads is cheap and efficient. Species that are not traditionally considered “model organisms” but await genome sequencing for comparative and functional genomics analyses are at last amenable to in-depth genome-wide analyses.

global carbon cycle. However, their saprotrophic activities also cause severe problems with the degradation of man-made products and in causing food spoilage. Mortality from human fungal pathogens has increased in recent years, especially in immunocompromised patients. In plants, ~90% of diseases are caused by fungi, and these result in massive losses in crop yield worldwide, with often profound socio-economic effects, sometimes resulting in severe famines [3]. Nevertheless, fungi also have beneficial effects in symbioses, such as mycorrhiza (fungus/plant root) and lichen (fungus/algae) associations. Greater than 80% of terrestrial plants have mycorrhizal relationships with fungi that allow the plants to access key nutrients such as nitrogen and phosphorus from the soil [4]. Fungi are also of great importance in biotechnology, e.g. in the production of drugs and enzymes [5,6]. In addition, many fungi can be easily cultured and are amenable to microbiological, genetic, and molecular techniques. Therefore, fungi were some of the earliest model organisms for the study of genetics, biochemistry, cell and developmental biology. It is thus not surprising that the first eukaryotic organism for which a complete genome sequence was obtained is a fungus, the budding yeast *Saccharomyces cerevisiae* [7]. Today, fungi are the eukaryotic group with the greatest number of completely, or nearly completely, sequenced genomes (<http://www.ncbi.nlm.nih.gov/genomes/leuks.cgi>, [2]). This is not only owing to their ecological, medical, agricultural, biotechnological and economic significance, but also due to the fact that with a size of 10–90 Mb and 4,700–17,000 predicted genes, fungal genomes are among the smallest and most compact eukaryotic genomes known.

The sequences for almost all sequenced eukaryotic genomes have been obtained by conventional Sanger sequencing technology. Over the past five years “next-generation sequencing” techniques have revolutionized large-scale sequencing projects because of massively increased throughput, resulting in much reduced costs per base [8]. One major disadvantage of the current techniques is that none of them delivers read lengths that approach conventional Sanger technology: whereas Sanger sequencing

routinely yields 900 nt, the longest next-generation reads obtained are in the range of ~450 nt for Roche/454 pyrosequencing (from now on abbreviated as 454 sequencing), and the techniques with the highest throughput are with 36–80 nt still well below this. Short reads, e.g. as obtained by Illumina/Solexa sequencing (from now on abbreviated as Solexa sequencing) cause severe difficulties for the assembly of genome sequences that contain repetitive sequences, as is the case for many higher eukaryotes. Thus, next-generation sequencing techniques have so far mostly been used for the *de novo* sequencing of prokaryotic genomes or the re-sequencing of eukaryotic species with reference genomes, where the next-generation reads can be mapped on an existing genome sequence [8–11]. Recent improvements, e.g. paired-end sequencing (reads from matched ends of longer DNA fragments) and a steady increase in read length should make the *de novo* assembly of high-quality eukaryotic genomes possible. For example, the genome of the filamentous fungus *Grosmannia clavigera* was assembled from a combination of Sanger, 454, and Solexa sequence data [12] and a first draft of the 2.4 Gb Giant Panda genome has been assembled from Solexa sequence reads alone [13]. Because of their small size, fungal genomes are perfectly suited for the task of optimizing *de novo* assembly approaches to generate high-quality or even finished larger eukaryotic genomes.

Here, we present the *de novo* assembly and annotation of the genome sequence of the filamentous fungus *Sordaria macrospora*. The genome was sequenced solely by next-generation techniques (Solexa sequencing by synthesis and 454 pyrosequencing). *S. macrospora* is an ascomycete with a long-standing history as a model organism for fungal sexual development and meiosis [14–18] (Figure 1). Development of a large set of genetic tools for this fungus [19–24] resulted in the discovery of novel proteins involved in central events of meiosis and organogenesis [25–32]. Similar to its close relative *Neurospora crassa*, *S. macrospora* is haploid with a nuclear genome of seven chromosomes and an estimated 39.5 Mb of DNA sequence [24,33–35]. Previous studies found ~90% nucleic acid identity within coding regions of orthologous genes from *S. macrospora* and *N. crassa* as well as a high degree of synteny over large genomic regions [36,37]. Despite their close phylogenetic relationship, *S. macrospora* is homothallic (self-fertile) in contrast to the heterothallic (self-sterile) *N. crassa*. The natural habitat of *S. macrospora* is herbivore dung in temperate climates, whereas *N. crassa* is usually found on burned vegetation and the soil throughout the world [14,38–41]. Thus, these two closely related fungi have evolved different life styles and inhabit different ecological niches. These differences may be at least partially reflected in their genomes.

The *S. macrospora* genome sequencing project had two aims: (1) to assemble a first, high-quality draft of the genome sequence after next-generation sequencing to show that this approach is feasible for filamentous fungi in general, and (2) to annotate the genome sequence by a community effort, with the goal of a better understanding of *S. macrospora* biology and the idea of improving its value as a model organism for fungal development.

Results/Discussion

Sequencing and assembly of the *S. macrospora* genome

The genome of the *S. macrospora* strain k-hell was sequenced by a combination of Solexa and 454 sequencing. First, a total of 3.4 Gb of DNA sequence in 95,153,034 Solexa 36-nt reads were obtained from one single-read lane (9,688,226 reads), four lanes of paired-end reads (55,337,284 reads) from a 300-bp insert library, and three lanes (30,172,524 reads) of paired-end reads from a 500-bp insert library (Table 1, Figure S1). This represents 85-fold

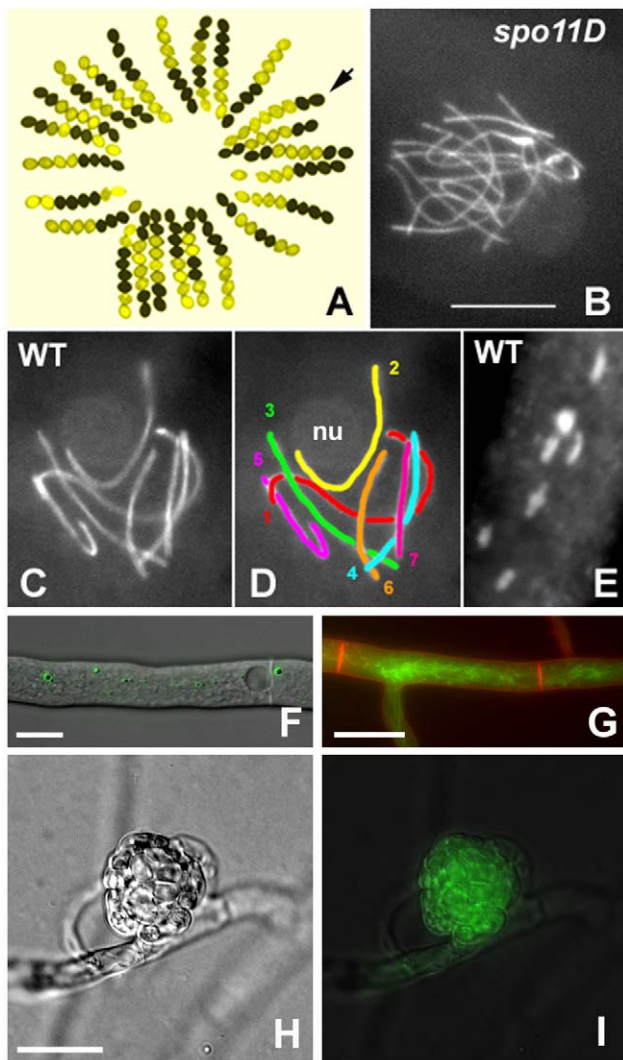


Figure 1. *S. macrospora* as a model organism for the analysis of meiosis and fruiting body development. (A) Segregation of the ascospore-color mutant *pam2* from a cross; wild type (black ascospores) by *pam2* (yellow ascospores). Arrow points to a gene conversion indicated by two black and six yellow ascospores. (B–D) Meiotic prophase. Chromosome axes are stained by the cohesin-associated Spo76/Pds5 protein tagged with GFP. (B) Prophase nucleus of a *spo11* null mutant: the 14 chromosomes do not align or synapse and this asynaptic status is seen from leptotene through pachytene. (C, D) Pachytene nucleus from wild-type *Sordaria*: the seven bivalents are differentiated by their size (D). Chromosome 2 (yellow), which bears the nucleolar organizing region, is attached to the nucleolus (nu). (E) The seven bivalents at late diplotene, stained by DAPI. Note the difference in size when compared to the pachytene nucleus. Bar (B–E) = 5 μ m. (F) An EGFP-HEX1 fusion protein localizes to Woronin bodies. Bar = 10 μ m. (G) The GFP-tagged developmental protein PRO41 localizes to the endoplasmic reticulum. Plasma membrane stained with FM4-64. Bar = 10 μ m. (H, I) In a young protoperithecium (H), the GFP-tagged developmentally induced protein APP accumulates (I). Bar = 20 μ m. doi:10.1371/journal.pgen.1000891.g001

coverage of the *S. macrospora* genome. Assembly of the Illumina/Solexa data with the Velvet assembler [42] resulted in 38.7 Mb of sequence data in 3,344 contigs with an N50 size of 51 kb (Table 2). As expected, these contigs contained a substantial number of internal gaps (17,956 gaps, Table 2), because paired-end data allows contigs to be scaffolded by inferred physical linkage of the matched pairs in the absence of contiguous coverage of

Table 1. Main features of primary sequence data.

primary sequence data	Solexa	454	Solexa +454
no. of reads that were obtained	95,153,934	1,103,372	96,261,736
read length	36 nt	367 nt ¹	n.a.
total length of all sequence reads	3,426 Mb	415 Mb	3,879 Mb

¹ average read length.

doi:10.1371/journal.pgen.1000891.t001

intervening segments. Despite the internal gaps in some of the contigs, we decided not to call them scaffolds to differentiate between the Velvet output (referred to as contigs even when containing gaps) and a subsequent scaffolding step (see below). When compared with the *N. crassa* genome, we were able to map 8,350 of ~10,000 predicted proteins to the 10,066 predicted *N. crassa* genes (e-value $\leq 10^{-20}$) which is only slightly lower than the number obtained with the final high-quality draft (8,519 proteins, see below). Thus, even this preliminary assembly covered most of the protein-coding genome.

To close most gaps, we obtained additional sequence data by 454 sequencing. Because of longer reads, a relatively low coverage with 454 reads in combination with the previously obtained Solexa reads was expected to allow assembly with a higher N50 value and close internal gaps in the contigs. We obtained 415 Mb (~10-fold coverage) of single-end 454 reads with an average read length of 367 bp (Table 1, Figure S1). Assembly of 454 reads only (with the Celera Assembler 5.3; Eurofins MWG GmbH, Ebersberg, Germany) yielded 14,123 contigs (N50 size 11 kb; 1,681 internal gaps; Table 2). Gaps in this assembly were primarily caused by sequencing ambiguities.

The combined raw data (Solexa and 454 reads) and the pre-assembled 454 data were used for constructing an assembly with the Velvet assembler version 0.7.31 [42] (Figure S1). This resulted in an assembly of 39.9 Mb of sequence data (5,097 contigs with an N50 size of 117 kb) and only 624 internal gaps within the contigs (Table 2). Thus, the combination of Solexa paired-end reads with 454 reads resulted in an increase of the N50 value and a drastic reduction in the number of gaps compared to assemblies where each data set was used alone. With a size of 39.9 Mb, this combined assembly corresponds well to previous analyses of the *S. macrospora* genome by pulsed-field gel electrophoresis that estimated the genome size at 39.5 Mb [24].

To determine whether similar results might be obtained with fewer sequence reads, thereby further decreasing sequencing costs, we generated test assemblies with different combinations of coverage levels (Figure S2, Table S1). The addition of 454 reads had the most drastic effect on the number and length of gaps whereas addition of paired-end reads improved mostly the N50 value. The inclusion of fewer sequence reads resulted in suboptimal assemblies; however, at the number of reads used for our assembly, bench mark values were no longer changing dramatically, suggesting that a plateau had been reached where addition of this type of sequence reads did not significantly improve assemblies. Further improvement might be achieved by sequencing paired-end libraries with longer inserts. The genome sequence of the filamentous ascomycete *Grossmannia clavigera* was assembled from a combination of Sanger paired-end reads (0.3-fold coverage), 454 single reads (7.7-fold coverage), and Solexa paired-end reads (100-fold coverage) [12], resulting in a high-quality draft genome sequence of 32.5 Mb with an N50 size of 164 kb. Our data show that similar values can be obtained even

Table 2. Main features of *S. macrospora* genome assemblies from Solexa reads, 454 reads, a combination of both, and after comparative assembly with the *N. crassa* genome.

assembled genome	Solexa	454	Solexa +454	comp. assembly
N50 value of assembly ¹	51 kb	11 kb	117 kb	498 kb
maximum contig/scaffold length	267 kb	64 kb	991 kb	2.5 Mb
total length of assembly	38.7 Mb	42.1 Mb	39.9 Mb	39.9 Mb
no. of contigs/scaffolds	3,344	14,123	5,097	4,781
% of assembly in contigs >0.5 kb	99.1	95.6	98.1	98.1
% of assembly in contigs >10 kb	92.8	52.5	92.3	93.1
no. of gaps within contigs	17,956	1,681	624	933 ²
mean length of gaps	478 nt	1 nt	21 nt	150 nt ²

¹ The N50 is defined as the length for which 50% of all bases in the assembly are in a contig of at least that length. In other words, this means that 50% of the assembly is contained in contigs of at least the N50 length.

² The higher number and greater length of gaps in the comparative assembly compared to the Solexa+454 assembly stems from the introduction of gaps while joining contigs to scaffolds.

doi:10.1371/journal.pgen.1000891.t002

without including Sanger sequencing data thereby drastically decreasing sequencing costs.

It has been previously demonstrated that several regions of up to 50 kb of the *S. macrospora* genome are syntenic to *N. crassa* [36,37]. To extend this analysis to the newly assembled *S. macrospora* contigs, the five largest contigs from the Velvet assembly (519–991 kb) were compared to contigs of the *N. crassa* finished genome that have been assigned to specific linkage groups by mapped genetic markers (Assembly 9; <http://www.broadinstitute.org/annotation/genome/neurospora/Regions.html>). The results were visualized as dot plot (Figure 2A), and show that each contig maps to one or two linkage groups with only one to three breaks of synteny. Thus, the high degree of synteny between *S. macrospora* and *N. crassa* that was expected from previous studies was reflected in the Velvet assembly. To make use of this high degree of synteny and further improve the *S. macrospora* assembly, we generated a comparative assembly with Mercator by using the scaffolded chromosomes of the draft *N. crassa* genome (assembly 7, [43]) and the draft-sequences of the *Neurospora discreta* (<http://genome.jgi-psf.org/Neudi1/Neudi1.home.html>) and *Neurospora tetrasperma* (<http://genome.jgi-psf.org/Neute1/Neute1.home.html>) genomes to order and scaffold the *S. macrospora* contigs [44]. This resulted in a total of 152 scaffolds and 4,629 contigs with an N50 size of 498 kb (Table 2). Syntenic regions between the *S. macrospora* and *N. crassa* genomes were analyzed by dot plot analysis (Figure 2B). To verify that the scaffolded contigs represent the correct order within the *S. macrospora* genome, three regions spanning gaps between contigs on scaffolds 17, 58, and 98, respectively, were amplified by PCR and sequenced. In all cases, sequences between 0.8 and 1.2 kb were retrieved that close the gap between adjacent contigs thereby validating the scaffolding results (data not shown). This assembly represents the first high-quality draft version of the *S. macrospora* genome (“*S. macrospora* assembly 1”, acc. no. CABT01000001-CABT01004783, http://gb2.fungalgenomes.org/gb2/gbrowse/sordaria_macrospora).

Neither the rDNA repeat units nor the mitochondrial genome was represented in the Velvet assembly. We therefore searched the raw data as well as preassembled 454 and Solexa contigs for sequences with significant identity to rDNA or mitochondrial DNA from other fungi (Text S1). These reads were used to assemble both one rDNA unit as well as the mitochondrial DNA using CodonCode Aligner version 3.0.3 (<http://www.codoncode.com/aligner/>). The rDNA unit shows ~98% DNA sequence

identity to that of *N. crassa*. Unlike in *N. crassa*, no additional smaller rDNA regions with point mutations were found by this method. Four shorter contigs had SNPs in various locations when compared to the full-length rDNA region. These SNPs all occurred as part of a homonucleotide run (4–6 nt), suggesting either sequencing errors or true polymorphisms in the rDNA repeats, which are considered to be rare in filamentous fungi but do exist in *N. crassa* because of the occurrence of RIP (see below; K.M. Smith and M. Freitag, unpublished data).

The mitochondrial genome encompasses 88.4 kb, and thus is larger than the 64.8 kb mitochondrial genome of *N. crassa* and smaller than the 94.2 kb mitochondrial genome of *Podospira anserina*. With 33.6%, the GC content of the mitochondrial genome is in the same range as that of *N. crassa* (36.1%) and *P. anserina* (29.9%) (Text S1, Figure S3). Our data show that not only the single copy regions of the nuclear genome can be assembled from the next-generation sequencing data, but also multi-copy regions like the rDNA unit and the mitochondrial genome, even if they are not initially recovered in typical Velvet runs.

Comparisons between closely related species reduce the number of orphan genes

Gene models for the first draft of the *S. macrospora* genome were predicted with four independent *ab initio* gene prediction programs trained on *N. crassa* and evidence-based predictions with *N. crassa* proteins (see Materials and Methods). The results were integrated with Evigan [45] to yield ~12,000 gene models. Additionally, 455 tRNA genes were predicted, similar to the 424 tRNA genes predicted for *N. crassa* [43]. The initially predicted ~12,000 protein coding genes were screened for ORFs with internal stops, lack of initiation or termination codons, unusually long introns and insufficient support by sequence similarity. Such ORFs were corrected or removed resulting in a refined gene set of 10,789 genes with an average length of 1,432 bp for all predicted coding sequences (CDS, Table 3, Table S2). The overall GC content of the genome is 52.4%. This is changed to 56.5% in coding regions, which represent 38.4% of the genome, and 49.8% in non-coding regions, which make up 61.6% of the genome.

To address the question of sequencing errors, we PCR-amplified and resequenced coding regions for six predicted genes (*SMAC_01188*, *SMAC_01198*, *SMAC_6009*, *SMAC_07685*, *SMAC_07776*, *SMAC_09680*) with frameshifts or internal stops. These were confirmed by resequencing in four cases, whereas in

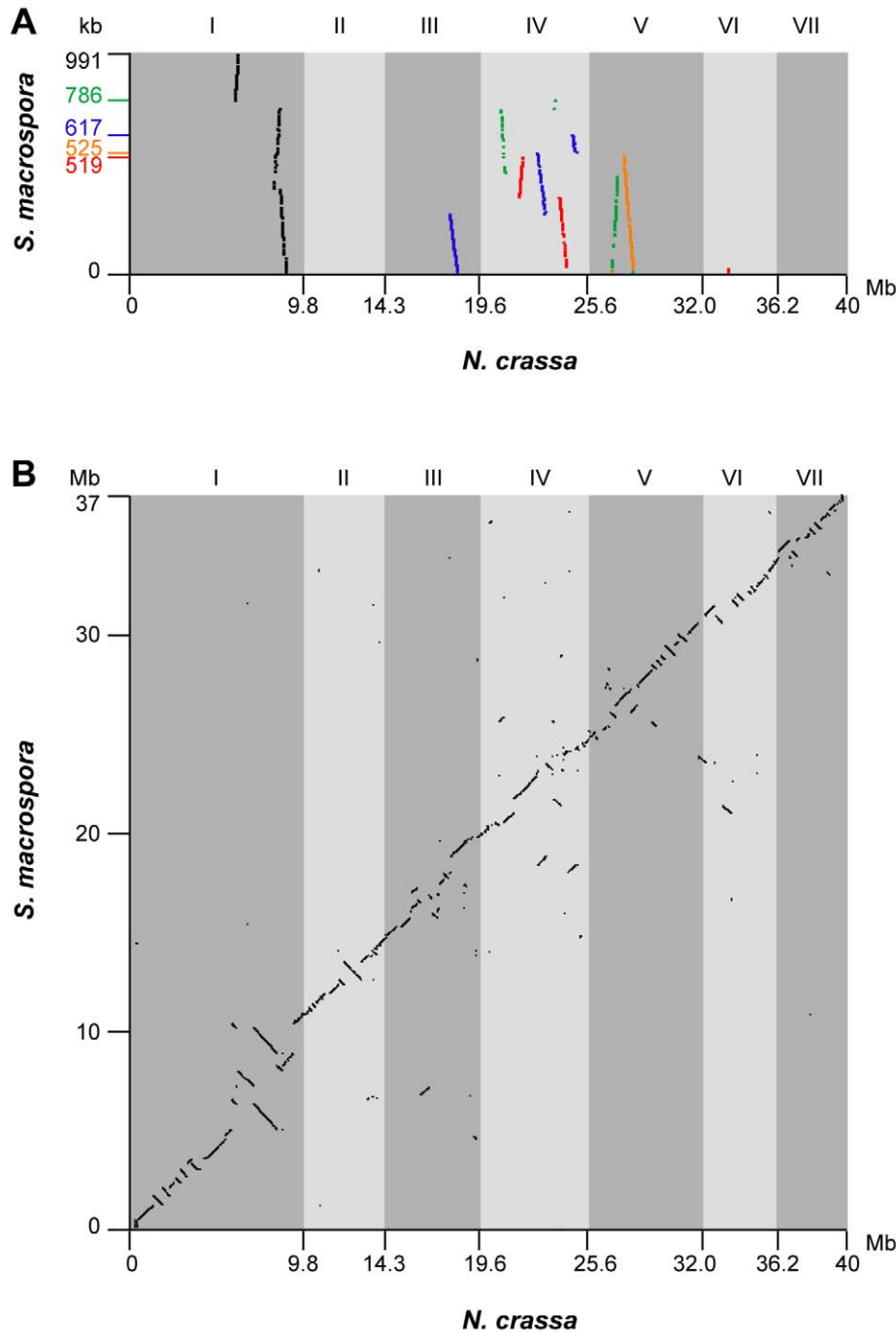


Figure 2. Synteny between the genomes of *S. macrospora* and *N. crassa*. (A) Synteny of contigs from the *S. macrospora* genome with the *N. crassa* genome before scaffolding along the *N. crassa* chromosomes. Dot plot of a comparison of the five largest contigs from the Velvet assembly (contigs 3467, 1588, 19727, 3369, and 12432, length given on the y-axis in descending order, total size of the five contigs 3.4 Mb, note that the Velvet contig numbers do not correspond to the contigs of the final assembly) against the Neurospora linkage groups (supercontigs I to VII in finished genome sequence, <http://www.broadinstitute.org/annotation/genome/neurospora/Regions.html>). The linkage group numbers for *N. crassa* are given above the dot plot. (B) Dot plot of a comparison of the *S. macrospora* scaffolds which cover 93% of the genomic sequence against the *N. crassa* supercontigs corresponding to linkage groups I to VII from the finished genome sequence. Comparisons for both analyses was done with BLASTN with $e\text{-value} < 10^{-150}$. Dot plot visualization was done with Combo [148]. doi:10.1371/journal.pgen.1000891.g002

two cases, insertions or deletions of 1 nt were found in the assembled sequence which when corrected led to the prediction of functional open reading frames. In total, we tested 21 kb of coding sequence by resequencing and found four insertion/deletion errors (0.02%). Although it is difficult to compare errors and error rates,

this rate is similar to the 0.1–0.001% error rates achieved in microbial draft genomes sequenced by Sanger technology [46,47].

With 10,789 predicted and partially curated genes, the gene count in *S. macrospora* is similar to that of *N. crassa* (10,066 community-annotated and centrally curated genes). To determine

Table 3. Main features of the *S. macrospora* genome sequence.

Size of the final assembly	39.8 Mb
chromosomes	7
GC percentage (total genome)	52.4
GC percentage in coding regions	56.5
GC percentage in non-coding regions	49.8
tRNA genes	455
protein coding genes (CDSs)	10,789
percent coding	38.4
average CDS size (min/max)	1,423 bp (54 bp/33,321 bp)

doi:10.1371/journal.pgen.1000891.t003

how many predicted proteins in these two closely related species are orthologs, reciprocal BLASTP analysis was performed: At an e-value of $\leq 10^{-20}$, 8,519 *S. macrospora* proteins have at least one homolog among the *N. crassa* proteins; *vice versa*, 8,179 *N. crassa* proteins have at least one homolog among the *S. macrospora* proteins. In total, 7,855 proteins (72.7% of all *S. macrospora* proteins) have reciprocal best hits in both searches identifying them as likely orthologs (Table S3).

Sequencing of the first few eukaryotic genomes revealed relatively high frequencies of “orphan genes” (i.e. genes without apparent homologs in any of the already known sequence databases and proteomes). As more genomes become available, this number has been rapidly decreasing, e.g. for *N. crassa* from ~41% [43] to currently 22% (2,219/10,066 [48]). Because *S. macrospora* is more closely related to *N. crassa* than any other previously sequenced filamentous fungus, we compared the *N. crassa* orphan genes with the *S. macrospora* genome using TBLASTN and BLASTP to assess how many proteins are lineage-specific (Table S4). Of 2,112 *N. crassa* orphan genes that were retrieved from the current *N. crassa* MIPS protein list (<http://mips.helmholtz-muenchen.de/genre/proj/ncrassa/>), 870 do not have significant hits in the *S. macrospora* genome at an e-value of $\leq 10^{-20}$. Orphan genes might comprise more quickly evolving genes [48], and we therefore repeated our analysis at an e-value $\leq 10^{-5}$. This analysis still left 471 (4.7%) genes without significant hits, suggesting that these genes may constitute the remaining true orphan genes that separate the genus *Sordaria* from *Neurospora* (Table S4). The recent sequencing of additional *Neurospora* species is expected to further reduce the number of genus-specific genes.

In addition to assessing the conservation of protein-coding gene regions, we sought to investigate the conservation of non-coding regions between *S. macrospora* and its closest relatives. Therefore, we performed comparisons of 5' upstream regions in 1 kb blocks from 1 kb to 4 kb as well as comparisons of introns and coding regions for *S. macrospora*, *N. crassa*, *N. discreta* and *N. tetrasperma* (Figure 3, Figure S4 and Table S5). We observed that introns are more conserved than upstream regions. Among the upstream regions, pairwise identity is slightly but significantly higher in the 1 kb upstream regions than in any of the other tested upstream regions (Table S5). This suggests that most regulatory (and therefore putatively conserved) elements in 5' UTRs and promoters reside within the 1 kb upstream regions.

We also compared the predicted *S. macrospora* proteins to the non-redundant GenBank and Swissprot databases (Table S2). Approximately 6% (631/10,789) of all predicted proteins did not

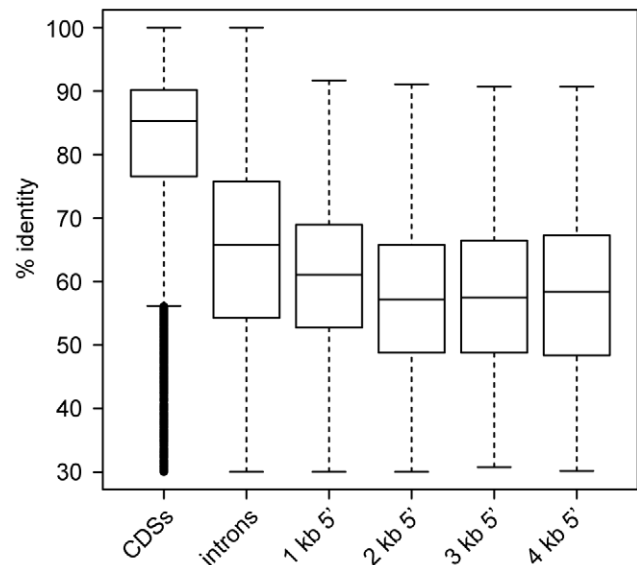


Figure 3. Pairwise identity between *S. macrospora* and *N. crassa* for different genomic regions. CDSs, introns, and regions upstream of CDSs (in 1 kb steps ranging from 1 to 4 kb) were used for comparison. Only those upstream regions were used that do not overlap with a protein coding region. Each region was used only once even if it is upstream of two divergently transcribed genes to avoid double-counting. The box plots show the distribution of % pairwise identities with the median value as a horizontal line in the box between the first and third quartiles. Detailed information on the comparisons can be found in Figure S4 and Table S5. doi:10.1371/journal.pgen.1000891.g003

have a significant hit against the non-redundant database at an e-value $\leq 10^{-5}$. This number is only slightly higher than that for *N. crassa* (4.7%, 471 genes, see above). Taking into account that no other *Sordaria* species have been sequenced yet, we suggest that the number of true orphan genes in ascomycetes might be less than 5% or 500 genes per genome.

A search for conserved protein domains in the predicted *S. macrospora* proteins was performed with the HMMER program hmmpfam [49,50] and with the InterProScan function from Blast2GO [51,52]. With HMMER, one or more conserved domains were found in 5,471 predicted proteins (50.7%, Tables S2 and S6), the InterProScan found domains in 7,099 predicted proteins (65.7%, Table S2). These values might seem rather low when compared to the more than 10,000 proteins that have a hit in the non-redundant database, but it reflects the fact that many (predicted, hypothetical or conserved hypothetical) proteins have not yet been functionally characterized; therefore many domains remain to be identified.

In addition to a comparison to *N. crassa*, an analysis of the predicted proteins from *S. macrospora*, *N. crassa*, *N. discreta*, *P. anserina*, and *Chaetomium globosum* was performed with OrthoMCL, a software that clusters orthologs and “recent” paralogs [53]. We identified 9,971 orthogroups, and among these 5,428 (54.4%) comprise single genes from each of the five species, i.e. single-copy genes that are conserved among all species investigated (Tables S7 and S8). 31 orthogroups contain genes with three or more paralogs in *S. macrospora*, but fewer or no paralogs in other fungi, and these were investigated further. Some of these orthogroups contained proteins suggestive of transposon activity (see below), whereas others have no homology to transposons or pseudogenes. Phylogenetic analysis of two orthogroups (99 and 79) indicates evolutionary histories of ancient gene family expansion and

subsequent differential gene loss (Figure 4). Orthogroup 99 comprises three genes from *S. macrospora* and two genes from *P. anserina*, whereas in the *Neurospora* species and *C. globosum*, only one gene is present. The genes from this orthogroup encode

putative P450 oxygenases, and one might speculate that these proteins are beneficial for a coprophilic lifestyle, because only the coprophilic fungi *S. macrospora* and *P. anserina* have retained more than one copy. A similar case of duplication and subsequent loss

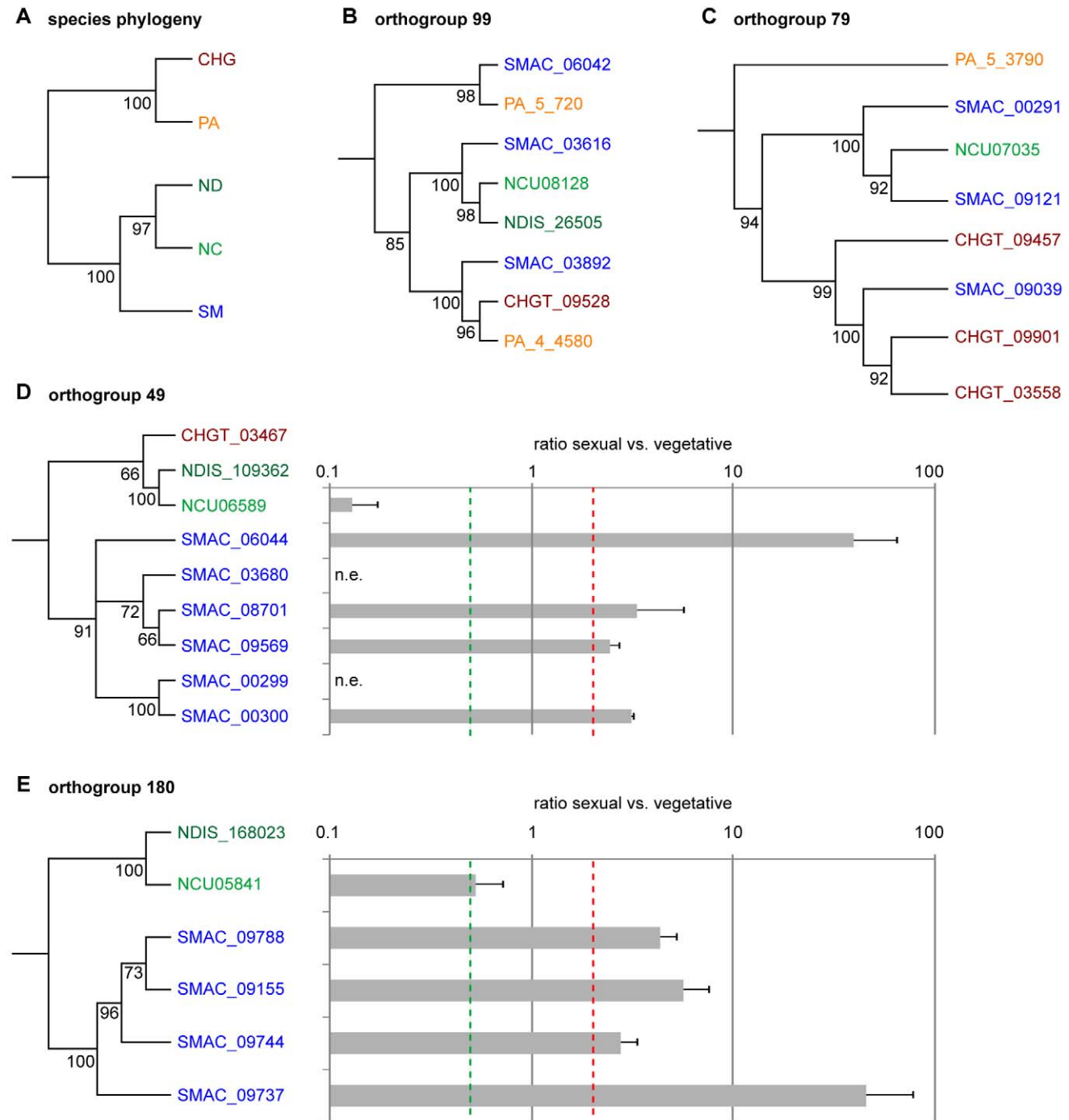


Figure 4. Phylogenetic analysis and expression of genes from different orthogroups from an OrthoMCL analysis of *S. macrospora* (SM), *N. crassa* (NC), *N. discreta* (ND), *C. globosum* (CHG), and *P. anserina* (PA). (A) Species phylogeny with six concatenated genes that are single-copy orthologs in each of the five species. (B–E) Phylogenetic trees with five different orthogroups. Outgroups for the trees were homologs from either *Nectria haematococca*, *Aspergillus fumigatus*, *Penicillium chrysogenum*, or *Pyrenophora tritici-repentis*. Numbers at branches indicate bootstrap support (10,000 bootstrap replications) in % for neighbor joining trees. (D–E) Expression of the *S. macrospora* and *N. crassa* genes from orthogroups 49 and 180 during sexual development compared to vegetative growth. Expression data are the results of two independent experiments and were determined by quantitative real time PCR. The red and green dashed lines indicate two-fold up- and downregulation, respectively. n.e., no expression was detected during vegetative growth or sexual development. doi:10.1371/journal.pgen.1000891.g004

can be postulated for orthogroup 79, which contains genes encoding chitin binding and glycosyl hydrolase domains.

In contrast, orthogroups 49 and 180 contain one or no gene for the *Neurospora* species, *P. anserina*, and *C. globosum*, but six and four members, respectively, in *S. macrospora*; and the *S. macrospora* genes cluster together in a phylogenetic tree (Figure 4). Thus, these genes seem to represent recent duplication events in *S. macrospora*. Both orthogroups are part of larger gene families, and to verify that placement of these subfamilies in different orthogroups was correct, an independent phylogenetic analysis was performed (Figure S5). This analysis supports the grouping by OrthoMCL. To test whether these genes are expressed genes and not simply annotation errors, quantitative real time PCR experiments were performed for ten *S. macrospora* genes from orthogroups 49 and 180 (Figure 4). For eight of the ten genes, transcripts were found under conditions of sexual development and/or vegetative growth, and all eight genes are upregulated during sexual development. In contrast, the homologous *N. crassa* genes are downregulated or not differentially regulated (Figure 4). Thus, the *S. macrospora* genes that are expressed under the conditions investigated might have gained developmental regulation after the split of the *Neurospora* and *Sordaria* lineages, probably as a result of gene family diversification after gene duplications. Whether these genes have a function during sexual morphogenesis in *S. macrospora* remains to be determined.

Repeated sequences, transposons, and genome integrity

Transposons and repeat elements have been identified in all eukaryotic groups investigated so far, and they can comprise large portions of a genome, e.g. 85% of the recently published maize genome [54,55]. In fungi they usually make up only a comparatively small part of the genome (usually $\leq 10\%$), because effective defense mechanisms against repeated sequences are in place and because smaller genomes are more streamlined [56]. Eukaryotic transposons can be divided into two classes, class I elements that transpose via an RNA intermediate, and class II

elements that transpose at the DNA level by excision and reintegration [57]. To analyze the transposon content of the *S. macrospora* genome, several approaches were used. First, amino acid sequences of known transposon open reading frames were used for comparison with the predicted *S. macrospora* peptides as described previously [58]. Second, DNA sequences of randomly selected scaffolds were compared to Repbase data [59]. These two approaches will identify only those repeated sequences or transposons that are similar to previously described elements. Third, DNA sequences of randomly selected scaffolds were compared to the complete genome sequence in order to identify new repeated sequences without similar entities in the databases.

Most interesting is the presence of five ORFs with amino acid sequence similarity to the *N. crassa* *Tad* LINE-like transposon [60] (Table 4). In addition, there are ~ 20 ORFs with sequence similarity to gypsy-type retrotransposons. However, these ORFs exhibit rather diverse sequences and do not form element families. In contrast to these class I elements, there are only three ORFs with similarities to class II eukaryotic transposons; two of these represent a *hAT*-like element [61] that we called “Scarce”, and one ORF with amino acid similarity to the *Fot1* transposon from *Fusarium oxysporum* [62]. As the only full-length Scarce ORF *SMAC_09680* contains a nonsense codon, it is likely that the element is no longer active, thus explaining the low copy number. Overall, the transposon load of *S. macrospora* is very low, much more resembling that of another homothallic fungus *Gibberella zeae* (anamorph *Fusarium graminearum*) [63] than that of *N. crassa*. This is also reflected in a search for regions of high similarity within the *S. macrospora* genome by performing a BLASTN analysis of the genome sequence versus itself (Figure S6). In this analysis, the prevalence of regions with high intragenomic similarity in *S. macrospora* is between those of *N. crassa* [43] and *F. graminearum* [63], all of which have significantly fewer intragenomic regions of high similarity than the repeat-rich genome of *Magnaporthe oryzae* [64]. This finding correlates well with the low transposon count of the *S. macrospora* genome. Taken together with the fact that we were able

Table 4. Repeated sequences and transposons in the *S. macrospora* genome.

class	superfamily	TSD	name	copies	ORFs
I	LINE	?	SmLINE1	5	<i>SMAC_00574</i> , <i>SMAC_00575</i> , <i>SMAC_09800</i> , <i>SMAC_09693</i> , <i>SMAC_01061</i>
I	gypsy	?	Sinti1 ¹	5	<i>SMAC_09594</i> , <i>SMAC_09832</i> , <i>SMAC_09794</i> , <i>SMAC_09714</i> , <i>SMAC_09614</i>
I	gypsy	?	Sinti2 ¹	15	<i>SMAC_01060</i> , <i>SMAC_09809</i> , <i>SMAC_09656</i> , <i>SMAC_09808</i> , <i>SMAC_09467</i> , <i>SMAC_10331</i> , <i>SMAC_09614</i> , <i>SMAC_09896</i> , <i>SMAC_09651</i> , <i>SMAC_06354</i> , <i>SMAC_10067</i> , <i>SMAC_09714</i> , <i>SMAC_09794</i> , <i>SMAC_07477</i> , <i>SMAC_09832</i>
II	hAT	?	Scarce	2	<i>SMAC_09680</i> , <i>SMAC_10246</i>
II	Fot1	?	—	1	<i>SMAC_04440</i>
?	—	5 bp	Smini1	60 ⁴	—
?	—	—	Smini2	34 ⁴	—
?	—	5 bp	Smini3 ²	80 ⁴	—
?	—	—	Smini4 ²	74 ⁴	—
?	—	—	Smini5 ³	14 ⁴	—

TSD: target site duplication present at least for some elements.

1 These elements show a very high degree of sequence variation; in addition Repbase analysis indicates additional DNA sequences with similarities to gypsy-like sequences.

2 Both elements exhibit partial sequence similarities.

3 Elements often inside ORFs or overlapping with ORFs.

4 Elements with at least 80% sequence similarity.

doi:10.1371/journal.pgen.1000891.t004

to assemble long contigs and that the assembly size correlates well with the genome size determined by pulsed-field gel electrophoresis, this suggests that the low repeat content is not an assembly artefact.

In addition to class I and II transposable elements, five different non-coding short repeat sequences (Smini1 to Smini5, 150–670 bp, Table 4) were detected. Two of these have partial sequence identity (Smini3 and Smini4) because of overlapping sequences. To verify that these repeats are real and not due to assembly problems, at least two copies for each repeat were PCR amplified and sequenced. For all tested repeats, their presence within the predicted genomic context was confirmed. Ten copies of repeat Smini5 are within ORFs, two are outside of ORFs, and another two overlap with ORFs. At least six of these ORFs show similarities to retrotransposon sequences. Some Smini1 and Smini3 repeats possess 5 bp target site duplications suggesting that they may be transposons or integrated elements caused by transposition. In some cases, point mutations may have modified target site duplications, or recombination may have occurred as has been shown for *Aspergillus niger* [65]. As Smini1 and Smini3 are both uniform in size (with the exception of some truncated elements), they may be solo-LTRs rather than mini-transposons such as the *guest* element of *N. crassa* [66]. Altogether, these five short repeat types cover only 56.8 kb of the genome (0.14%).

In *N. crassa* and a few other ascomycetes (e.g. *P. anserina* [67,68], *M. grisea* [69], *F. graminearum* [63], and *Leptosphaeria maculans* [70]), the RIP machinery detects pairs of repeated segments during premeiosis, introduces C:G to T:A mutations and can trigger DNA methylation of the mutated repeats in the vegetative cells resulting from ascospores, presumably by virtue of the increased AT content [71]. We analyzed the entire *S. macrospora* genome sequence for the presence of RIP footprints by calculating RIP indices [72] on the concatenated contigs and scaffolds (Figure S7). In contrast to the situation in *N. crassa*, where large regions mutated by RIP make up the centromeric DNA (K.M. Smith, L.R. Connolly and M. Freitag, unpublished data), we found no large blocks of AT-rich regions with the typical RIP bias (e.g., TpA/ApT >1.0). The only large region with atypical dinucleotide distribution was scaffold 0, which contains the mtDNA. Here, both TpA/ApT and (CpA+TpG)/(ApC+GpT) were close to 1, suggesting DNA composition more reminiscent of bacteria or budding yeast. Our results suggest the absence of large regions mutated by RIP in the *S. macrospora* genome. Previous analyses have shown that there is no active RIP in *S. macrospora* (Kück et al., unpublished data). However, an ortholog of the *N. crassa* *rid* gene, the only gene known to be important for RIP [73], is present in the *S. macrospora* genome (Table S9), indicating that *S. macrospora* might have been able to undergo RIP during some time of its evolution; alternatively, RIP may occur at such low levels that it is difficult to detect in typical transformation and selfing experiments. RID homologs are involved in sexual development in two other fungi, *Ascobolus immersus* [74] and *Aspergillus nidulans* [75], suggesting that the *S. macrospora* protein may carry out a function independent of RIP.

In *N. crassa*, two other genome defense mechanisms in addition to RIP have been identified, namely meiotic silencing by unpaired DNA (MSUD or “meiotic silencing”) and a form of RNAi (“quelling”) [76,77]. All *N. crassa* genes identified in these processes have orthologs in *S. macrospora* suggesting that *S. macrospora* might be able to perform different varieties of genome defense (Table S9). The fact that endogenous genes can be silenced via introduction of transgenic constructs that result in double-stranded RNA molecules indicates an active RNAi-like mechanism [78]. Nevertheless, transformants with ectopically integrated copies for

genes involved in meiosis (which might be subject of MSUD) or other processes (which might be subject to RNAi) have been successfully generated in different laboratories working with *S. macrospora* for years. Silencing of the resident and/or ectopically located gene functions has never been observed or described (e.g. [21,25,30,79,80]). This suggests that *S. macrospora* might possess gene silencing mechanisms but that they are perhaps less active, at least with respect to transgenes, than in *N. crassa*.

Apart from genome defense mechanisms, there are a number of conserved processes in eukaryotes that are involved in maintaining genome integrity and regulating genome activity at the chromatin level [81]. We annotated chromatin-associated proteins, histone modification proteins, genes involved in the structural maintenance of chromosomes as well as centromere and kinetochore proteins and found that *S. macrospora* contains essentially the same set of genes as *N. crassa* (Table S9). Like its close relative, *S. macrospora* has single genes for the histone H3 K9 methyltransferase (DIM5), the heterochromatin protein 1 (HP1) and the DNA methyltransferase DIM-2, suggesting that heterochromatin formation and DNA methylation in *S. macrospora* are similar to what has been observed in *N. crassa* [43]. Taken together, these data indicate that *S. macrospora* contains the typical, conserved eukaryotic machinery for genome maintenance. Despite the absence of active RIP, this fungus appears to prevent the spreading of transposons and other repeated sequences as indicated by the low content of these elements within the genome.

Genes for regulatory networks, signaling, meiosis, and development

Since the 1950s, *S. macrospora* has been used as a model system for the analysis of fungal sexual development and meiosis, and a number of developmental genes have been characterized at the molecular level [14,82]. We searched for genes known to be involved in development or in signaling cascades in *S. macrospora* and other fungi and found that *S. macrospora* contains homologs to all conserved genes as expected, further confirming the quality of the genome sequence.

Specifically, we looked for orthologs to known genes for fungal sexual development, meiosis, GTP-, phospholipid- and calcium-signaling, motor proteins, senescence, photoreceptors and light signaling (Tables S10, S11, S12, S13, S14). In the case of photoreceptor-coding genes, it was found that *S. macrospora* contains homologs to known or putative fungal photoreceptors (Table S10). *S. macrospora* is able to undergo sexual development both in the dark as well as under white light [83]; however, in the light perithecial necks of *Sordaria* and *Neurospora* species exhibit positive phototropism in order to aim the active discharge of ascospores away from the growth substrate [84,85]. In *N. crassa*, this photoresponse is mediated by the blue light photoreceptor WC-1 [84,86–88]. Photoresponses often involve multiple photoreceptors, e.g. photoreceptors for red and blue light are present in one protein complex in *A. nidulans* [89,90]. To test whether wavelengths other than blue light also play a role in regulating neck phototropism, we tested the photoresponse of *S. macrospora* to green and red light. Under red light, perithecial necks were oriented in random directions similar to that of perithecia grown in complete darkness, but perithecial necks showed a strong positive phototropism in response to green light (Figure S8). Our results suggest that perithecial neck phototropism in *S. macrospora* is regulated by blue light, similar to photoresponses in *N. crassa* [91], and additionally by green light, a response not yet observed in other fungi. The photoreceptors responsible for this phenotype remain to be uncovered; possible candidates are two putative rhodopsin-like green light photoreceptors (SMAC_02424 and

SMAC_06025) that are orthologs of ORP-1 and NOP-1 in *N. crassa*, respectively [81,92].

Senescence in fungi has been observed in the model organism *P. anserina*, in strains of *N. crassa* and *N. intermedia* [93,94], but not in *S. macrospora*. A search for homologs to genes that are known to be involved in the aging process in *P. anserina* revealed that for the majority of the genes clear homologs are present in *S. macrospora* (Table S11). This includes genes that are required for mitochondrial protein quality control, programmed cell death, DNA repair, ROS scavenging, mitochondrial dynamics, and respiration, among other processes. Two genes not identified in *S. macrospora* are the apoptosis-related genes *PaAif1* and *PaAmid2*. *PaAIF1* (apoptosis-inducing factor) and *PaAMID2* (AIF-like mitochondrion-associated inducer of death) are putative NADH oxidoreductases. In mammals, AMID is present in mitochondria, and its overexpression induces cell death [95]. The third protein that is missing in *S. macrospora* is the SAM-dependent O-methyltransferase *PaMth1*. An accumulation of this protein was detected in the mitochondria and in total protein extracts of senescent *P. anserina* wild type strains [96,97]. Investigation of substrate-specificity of the protein hints to a protecting role of this methyltransferase against the generation of reactive oxygen species [98,99]. While *PaMth1* overexpressing strains show a significantly elongated life span, *PaMth1* deletion strains are short-lived. However, *S. macrospora* does not show a restricted lifespan despite the lack of a *PaMth1* homolog, indicating that the aging process in *P. anserina* is not conserved in other members of the Sordariales, and that the *P. anserina* aging genes that are present in *S. macrospora* may function in other cellular pathways.

Fungi have long been used as model systems to study the molecular mechanisms of meiosis, and *S. macrospora* has played a prominent role in these investigations due to its simple sexual life cycle, large meiotic products (ascospores) and the production of an ordered tetrad of ascospores that allows the differentiation between pre- and postreduction segregation of alleles [14,82]. Comparison of the predicted *S. macrospora* genes with the *S. cerevisiae* and *Schizosaccharomyces pombe* genomes [100,101] allowed the identification of 92 “meiotic” genes. Reciprocal best hit BLASTP similarity searches against the predicted ORFs of *S. macrospora*, *N. crassa* and *P. anserina* showed that the 92 genes display orthologs in all three species (Table S15) [81,102]. Nine of the genes were already characterized in *S. macrospora* (Table S15). The most conserved proteins include enzymes that are implicated in the recombination process and the proteins involved in sister-chromatid cohesion. In contrast, structural proteins like the components of the synaptonemal complex (SC) are poorly conserved despite the fact that the SC is as conserved during evolution as meiosis itself. This is similar to findings in other groups of organisms, e.g. mammals and plants [103]. Remarkably, *S. macrospora*, *N. crassa*, and *P. anserina*, like other filamentous fungi [104] possess only the RecA ortholog RAD51 and lack a recognizable DMCI1, the meiosis-specific homolog of RAD51, thought to play an essential role in strand invasion [105]. The meiotic regulators are also poorly conserved (Table S15): among the three meiotic-specific transcription factors in yeast (Abf1p, Ume6p and Ndt80p) only an Ndt80p homolog is identifiable. Thus, *S. macrospora* has a conserved set of meiotic core genes whereas the regulators are more diverged, probably indicating life style-specific adaptations.

We also searched for genes that may be involved in GTP-dependent and/or phospholipid or calcium signaling as well as known fungal developmental genes and genes encoding motor proteins, and found for all groups that the gene content of the *S. macrospora* genome is similar to that of *N. crassa*, and thus in most

cases larger than that of *S. cerevisiae* (Tables S12, S13, S14). This shows that *S. macrospora* is a useful model organism for studying developmental processes because it contains the full repertoire of higher eukaryotic genes involved in signaling and regulatory networks. Nevertheless, there are several groups of genes where *S. macrospora* differs from other fungi and that warrant a closer look because they allow insights into fungal evolution and biology. These are described below.

Genes for conidiation and nonself recognition: a case of “cryptic” incompatibility?

Two features in which *S. macrospora* differs from its close relative *N. crassa* are the lack of both asexual spores (“mitospores” or conidia) and heterokaryon incompatibility reactions. Searches in the *S. macrospora* genome for conserved genes that are involved in these processes revealed that homologs for conidiation genes are present (Table S16). These homologs seem to encode functional proteins, as they are not enriched in missense or nonsense mutations. Furthermore, quantitative real time PCR analysis for orthologs of six genes involved in conidiation in *N. crassa* revealed that these genes are expressed both during vegetative growth and sexual development in *S. macrospora* (Figure S9). Of course, additional unknown genes that are essential for conidiation may be missing or mutated in *S. macrospora*. Another possibility is that *S. macrospora* is able to conidiate, but does not do so under laboratory conditions. This would be analogous to the situation of *Aspergillus fumigatus*, which was recently shown to undergo sexual development when grown under suitable conditions [106,107]. A third possibility, discussed below, might be that *S. macrospora* no longer produces conidia due to an unfavorable combination of heterokaryon incompatibility genes.

Filamentous fungi can undergo hyphal fusion (anastomosis, [108]) between individuals of different genotypes leading to the formation of a mycelium containing genetically different nuclei (heterokaryon). In many ascomycetes such as *N. crassa*, *P. anserina*, and *A. nidulans*, the viability of these heterokaryons is genetically controlled by a set of heterokaryon incompatibility (*het*) loci. A *het* locus can be defined as a locus at which heteroallelism cannot be tolerated in a heterokaryon [109], thus a fusion between two individuals that differ genetically at a *het* locus results in a nonself recognition reaction which leads to phenotypes ranging from inhibited, abnormal growth to cell death [110]. Heterokaryon incompatibility (HI) has been shown to prevent the spread of viruses and the exploitation of aggressive phenotypes and is believed to reduce the risk of resource plundering between individuals [111–114]. However, heterokaryon formation can also have benefits for the individuals involved, e.g. the formation of functional diploids and mitotic genetic exchange in the parasexual cycle [115].

Several *het* loci have been characterized at the molecular level, and a conserved region of about 150 residues has been identified within various HI proteins. This domain is termed the HET domain [116]. The parts of *het* genes not encoding the HET domain are highly polymorphic; they ensure nonself recognition and are evolving very rapidly whereas the HET domain triggers cell death [117]. In addition to *het* domain genes, several other genes function as *het* loci, among them the mating-type genes in *N. crassa*, which act as *het* genes during vegetative cell fusion but are required to be different during sexual cell fusion [118–120].

Vegetative incompatibility has not been observed in *S. macrospora* [35]. Nevertheless, *S. macrospora* harbors genes for homologs to known *het* genes in other fungi (Table S17). A rather surprising finding was that in the case of *het-c*, *pin-c*, and a *tol*-related HET domain gene, not one, but two closely linked copies for each of

these genes are present in the *S. macrospora* genome (Figure 5, Table S17). This is in contrast to all other filamentous ascomycetes which encode only one homolog of the *het-c* gene [121]. In addition to *het-c*, a second, closely linked HET domain-encoding gene named *pin-c* is essential for the HI reaction in *N. crassa*. It was shown that nonallelic genetic interactions between *het-c* and *pin-c* mediate nonself recognition while the severity of the HI depends on allelic interactions at the *het-c* locus [122]. In *S. macrospora*, the genomic region that is orthologous to the *het-c/pin-c* locus in *N. crassa* contains two copies of *pin-c* (*SMAC_07217* and *SMAC_07219*) and one full-length (*SMAC_07220*) and one partial (*SMAC_07218*) copy of *het-c* (Figure 5). BLASTP comparison shows that the two PIN-C proteins from *S. macrospora* differ from each other to about the same degree as the *N. crassa* PIN-C allelic variants differ from each other (data not shown). The *het-c/pin-c* region is inverted in *S. macrospora*, and the genes at the ends of the inverted region, *het-c* and *pin-c*, are duplicated. To exclude the possibility that this is an assembly error, we amplified by PCR and end-sequenced DNA fragments spanning the regions between *SMAC_07217* and *SMAC_07218*, between *SMAC_07218* and *SMAC_07219*, between *SMAC_07219* and *SMAC_07220*, and between *SMAC_07220* and *SMAC_07229*. In all cases, we obtained PCR fragments of the expected size and sequence thereby validating that this gene order is not an assembly error but represents the wild type situation. Interestingly, the intergenic region between *SMAC_07217* and *SMAC_07218* contains two copies of the Smini1 repeat; thus, the duplication in this region may have originated from a transposition event. Phylogenetic analysis of the duplicated PIN-C homologs and the duplicated TOL-related proteins indicates that for *pin-c*, the duplication arose after the divergence of Sordaria from Neurospora, because the two *pin-c* copies are more similar to each other than to either of the three known *pin-c* alleles from *N. crassa* (Figure 5).

In *N. crassa*, two copies of *het-c* are only present in one cytoplasm after heterokaryon formation, and it has been shown that HET-C proteins encoded by different *het-c* alleles form a heterodimer complex at the plasma membrane during the HI reaction [123]. Thus, with respect to *het-c* and *pin-c*, the genomic situation in *S. macrospora* resembles that of a heterokaryon in *N. crassa* (Figure 6), but no obvious signs of HI, e.g. compartmentalization and cell death, are evident in *S. macrospora*. However, mild HI reactions in *N. crassa* can lead to less severe phenotypes, e.g. aconidial strains [124–127]. In *S. macrospora*, the second *het-c* copy is incomplete and the ortholog of *het-6*, another gene involved in HI in *N. crassa*, contains internal stop codons so that a full HI reaction might be prevented by only partially functional *het* genes. Thus, we hypothesize that the lack of conidiation in *S. macrospora* may be due to “cryptic” or “mild” HI caused by the presence of more than one copy of putative HI genes in the genome (Figure 6). However, as indicated above, this is just one of several hypotheses to explain the fact that *S. macrospora* is aconidiate despite possessing orthologs to all known conidiation genes.

Another point worth considering is that *S. macrospora* is homothallic and encodes mating type genes in one locus that are present in separate mating-type idiomorphs in *N. crassa* [128]. This situation would result in severe HI in vegetative cells of *N. crassa* mediated by the TOL protein. Only in *tol* mutants both mating type idiomorphs are tolerated in one vegetative cytoplasm [120]. Introgression of the *N. crassa tol* into *N. tetrasperma* caused HI and disrupted the pseudohomothallic nature of this fungus indicating that the native *N. tetrasperma tol* does not mediate HI [129]. Interestingly, the *S. macrospora TOL*, *SMAC_08253*, has only 40% amino acid identity to its *N. crassa* ortholog, an extremely low value compared to the average 89% identity in coding regions at

the DNA level [37]. Probably this very divergent TOL does not mediate HI and allows co-existence of all mating type genes within vegetative cells. Thus, HI in *S. macrospora* might be attenuated (“cryptic” HI) or abolished by mutations in critical HI-mediating genes to cope with or allow the presence of otherwise incompatible genes within one genome.

A second genomic locus that is important for HI in *N. crassa* and *N. tetrasperma* contains the *het-6* and *un-24* (*rnr-1*) genes. In this case, the two known alleles, Oak Ridge (OR) and Panama (PA), of both genes in both species differ not only in the sequences of the alleles, but also in the gene order within the *het-6/un-24* locus, which was caused by an inversion of a block of five genes including *un-24* [116,130,131]. An analysis of the orthologous region in *S. macrospora* revealed the same gene order as in the OR allele (Figure S10A). Phylogenetic analysis of both genes showed that the different allelic versions of *N. crassa* and *N. tetrasperma* cluster together as has been shown previously [131], while the *S. macrospora* genes occupy a basal position relative to the two *Neurospora* species (Figure S10B). This suggests that the OR allele represents the ancient gene order, and that the PA allele arose from an inversion after separation of Sordaria and Neurospora, but before speciation of *N. crassa* and *N. tetrasperma*; otherwise one would have to postulate two independent inversion events of the same genomic region leading to the OR gene order which is rather unlikely.

Some genes for secondary metabolism may have been acquired by horizontal gene transfer

Polyketides and non-ribosomal peptides are the most prominent classes of fungal secondary metabolites [6]. They comprise a wide variety of chemical structures, and a number of them have pharmaceutical applications, but their biological functions remain largely unknown [132,133]. Most filamentous fungi harbor several genes encoding polyketide synthases (PKS) as well as non-ribosomal peptide synthases (NRPS) in their genomes. Apart from the *pks* and *nrps* genes, the biosynthesis of a polyketide or non-ribosomal peptide usually requires additional genes that encode, for example, enzymes that modify the products of the PKSs and NRPSs. These genes are often clustered together with the corresponding *pks* or *nrps* gene within the genome [134]. In order to determine the potential of *S. macrospora* for the biosynthesis of secondary metabolites, we searched the predicted proteins for the occurrence of typical domains associated with PKS or NRPS proteins, and additionally also for fatty acid synthase (FAS) proteins as these have structural similarity to PKS proteins (Table S18). *S. macrospora* contains three putative *nrps* genes, three genes that fall into the *fas* class, and eleven putative *pks* genes. The numbers of *nrps* and *fas* genes are the same as in *N. crassa*, and the corresponding genes in the two fungi are orthologs. However, of the predicted eleven *pks* genes, only seven have an ortholog in *N. crassa*, whereas four PKS proteins have a higher sequence identity to other, more distantly related fungi. The *N. crassa* genome contains only eight putative *pks* genes one of which has no ortholog in *S. macrospora* [36,135]. Thus, with respect to *pks* genes and putative polyketides, *S. macrospora* appears to possess a greater potential for the production of secondary metabolites than its close relative *N. crassa* (Table S18, Figure S11).

Most of the *S. macrospora* polyketide biosynthesis genes that have been studied previously have been found to be upregulated during sexual development, and polyketides may play a role in fruiting body formation in *S. macrospora* [36,78]. Therefore, we determined the expression of the remaining five *pks* as well as the three *nrps* genes during sexual development (Figure 7). The *nrps* genes as well as eight of the eleven *pks* genes are transcriptionally upregulated

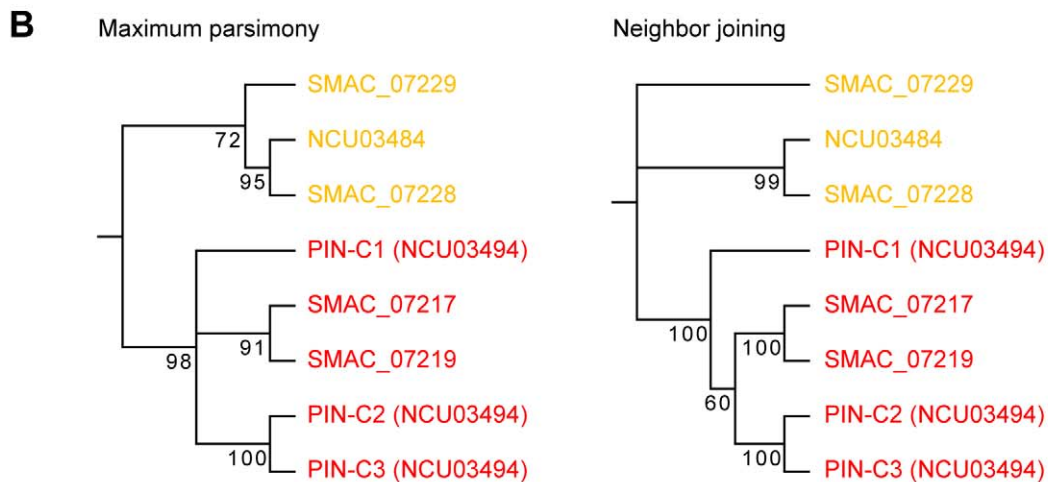
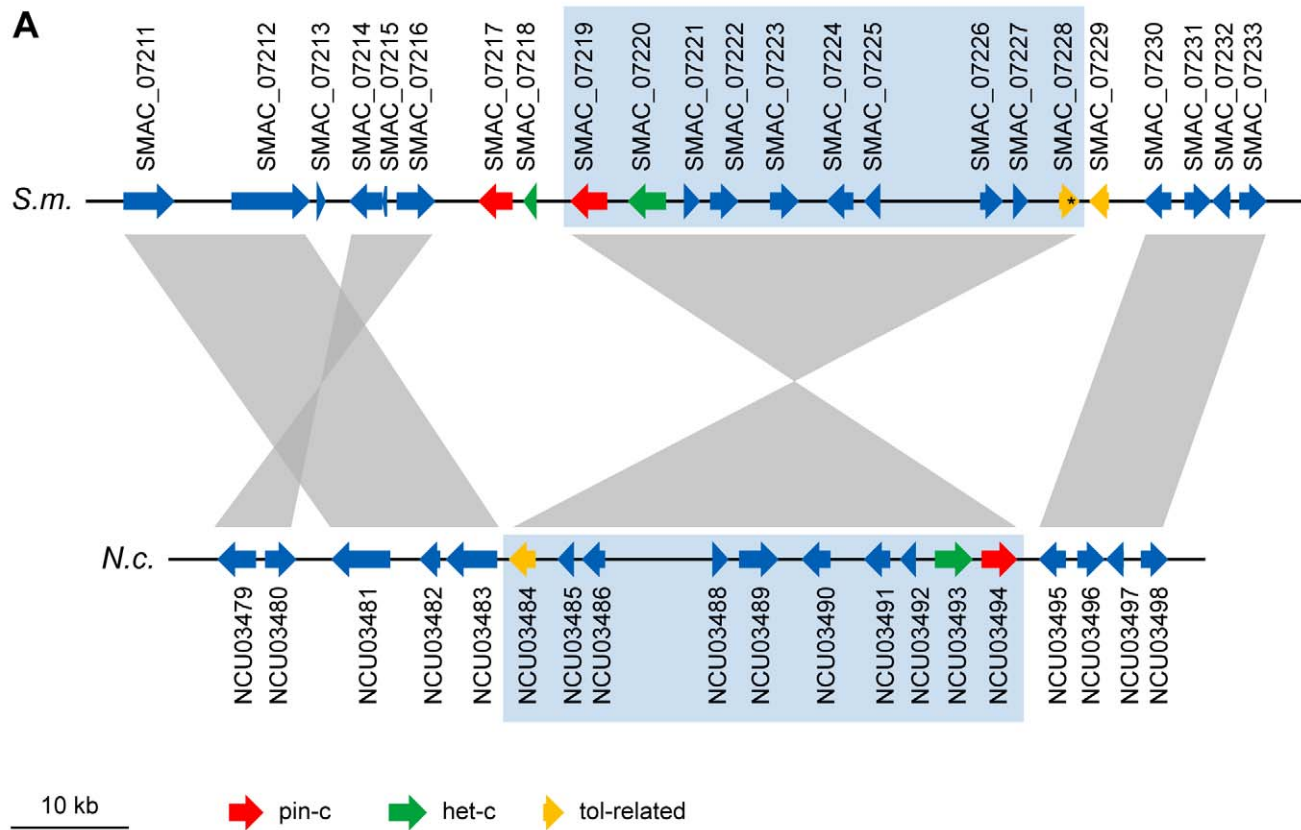


Figure 5. The *het-clpin-c* locus of *S. macrospora* contains additional copies of putative heterokaryon incompatibility genes. (A) Region from *S. macrospora* scaffold 98 and *N. crassa* contig 8 containing *het-c* and *pin-c* genes. A syntenic region containing the *N. crassa* *het-c* and *pin-c* genes and the orthologous region in *S. macrospora* is shaded in blue. In *S. macrospora*, this region is bordered by additional copies of *pin-c* and a partial *het-c* (left) and a TOL-related protein encoding gene (right). The *tol*-related gene *SMAC_07228* contains an internal stop codon within the open reading frame (indicated by an asterisk) and therefore encodes a shortened TOL-related protein or is a pseudogene. (B) Phylogenetic tree of PIN-C and TOL-related proteins from the genomic region shown in (A). For *N. crassa*, three allelic variations of PIN-C (PIN-C1, PIN-C2, and PIN-C3) were used for tree construction. The PIN-C1 protein from *Pyrenophora tritici-repentis* was used as an outgroup to root the tree. Maximum parsimony and neighbor joining trees were calculated with 10,000 bootstrap replications each. The phylogenetic tree separates the PIN-C and TOL-related proteins, however, it is not conclusive with respect to the putative ancestral state of the PIN-C alleles.

doi:10.1371/journal.pgen.1000891.g005

during sexual development. The three *pks* genes that are not upregulated comprise the single type III *pks* gene as well as two *pks* genes without orthologs in *N. crassa*. These two *pks* genes,

SMAC_01188 and *SMAC_01198*, are organized in a cluster of putative polyketide biosynthesis genes (Figure 8). Despite the fact that polyketide biosynthesis genes are often clustered in filamen-

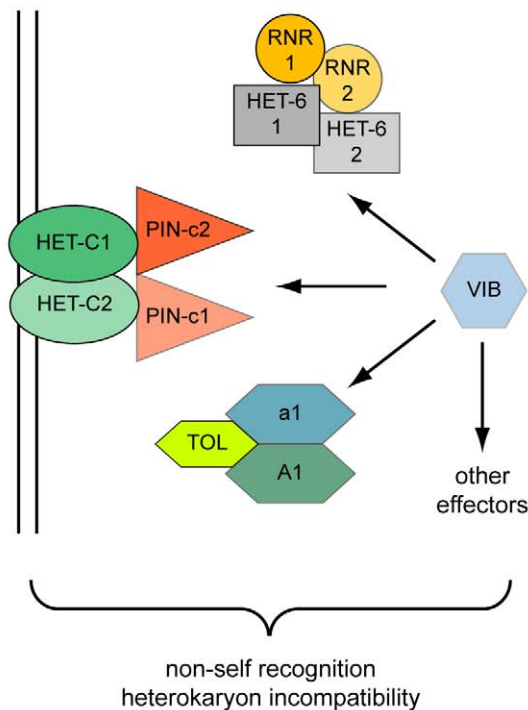
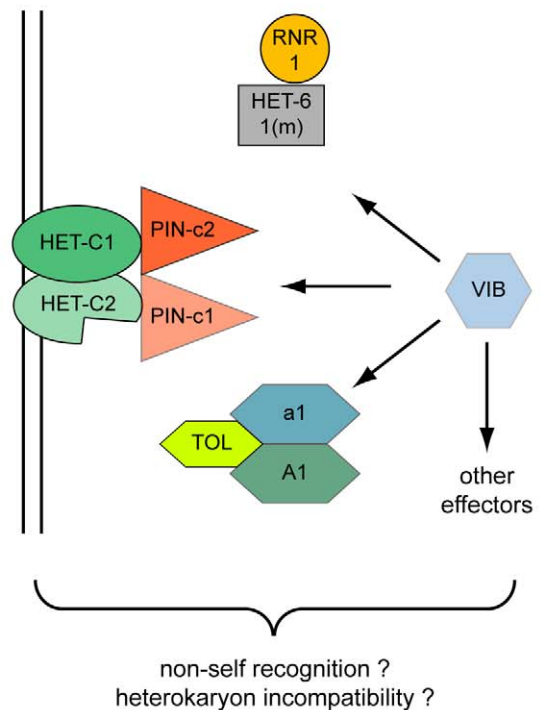
A *N. crassa*, two individuals**B** *S. macrospora*, one individual

Figure 6. Model for the action of heterokaryon incompatibility. Incompatibility in two incompatible strains of *N. crassa* (A) and in a single strain of *S. macrospora* (B). The VIB transcription factor regulates the expression of HET-domain genes *tol*, *het-6*, and *pin-c* [170]. The *het-6* gene of *S. macrospora* is mutated (m) and the second *het-c* gene (*het-c2*) is incomplete.
doi:10.1371/journal.pgen.1000891.g006

tous fungi [134], in *S. macrospora* only one such cluster has been found [36], and the genome sequence shows that most *pks* genes of *S. macrospora* do not occur clustered with other polyketide biosynthesis genes.

Apart from them being clustered, the two *pks* genes *SMAC_01188* and *SMAC_01198* are interesting because they do not have orthologs in *N. crassa* or any of the other sequenced Sordariomycete genomes (*P. anserina*, *C. globosum*, *F. graminearum*, *M. grisea*). This is true for most of the genes from the cluster spanning the region from *SMAC_01188* to *SMAC_01201* (Table S19). With the exception of *SMAC_01192* and *SMAC_01197*, the clustered genes do not have identifiable homologs within the Sordariomycetes, rather their most similar homologs are found within the Eurotiomycetes (*Aspergillus*, *Neosartorya*, *Penicillium*) or Dothideomycetes (*Phaeosphaeria*). In the center of the cluster, six genes are orthologs to genes from a putative polyketide biosynthesis cluster of *Phaeosphaeria nodorum* (Figure 8, syn. *Stagonospora nodorum*, http://www.broadinstitute.org/annotation/genome/stagonospora_nodorum/Home.html [136]). There are two likely explanations for these findings: (1) the cluster originated through gene duplication in a common ancestor of the Sordariomycetes and Dothideomycetes, and later on, massive gene loss occurred in the Sordariomycetes with the exception of *S. macrospora*; (2) *S. macrospora* acquired the cluster through horizontal gene transfer (HGT). To examine these two possibilities, we determined the sequence identity between the *S. macrospora* cluster proteins and their orthologs in the *P. nodorum* cluster as well as the sequence identity between all homologous *S. macrospora* and *P. nodorum* proteins, and found that the sequence identity between the

proteins from the cluster is significantly higher (Figure 8B). This is also the case when looking at the sequence identity of proteins with the same domains as the orthologs in the cluster.

A phylogenetic analysis was performed with the cluster protein *SMAC_01196* that encodes a putative phenylalanine ammonia lyase (PAL), a second PAL protein *SMAC_05651* present in *S. macrospora*, and the homologs from seven other fungi (Figure 9). As expected, *SMAC_05651* groups with the corresponding proteins from the Sordariales *N. crassa*, *C. globosum*, and *P. anserina*, each of which encodes only one PAL protein in their genomes. However, the “additional” PAL protein *SMAC_01196* from the cluster groups among the Leotiomycetes/Dothideomycetes proteins and is closest to the *P. nodorum* cluster protein *SNOG09914*. Phylogenetic analysis of the cluster protein *SMAC_01190* that encodes a putative member of the UbiA prenyltransferase family, its two other *S. macrospora* paralogs, *SMAC_02313* and *SMAC_06375*, and the homologs from eleven other fungi gives a similar picture: *SMAC_02313* and *SMAC_06375* group within the Sordariales, whereas *SMAC_01190* groups with the *P. nodorum* protein *SNOG_09915* within a section of the tree that contains proteins from the Dothideomycetes, Eurotiomycetes, and Leotiomycetes, but not Sordariomycetes (Figure S12).

The findings of (1) a conserved cluster of genes with closest homologs from the Dothideomycete *P. nodorum* instead of members of the Sordariomycetes, (2) the significantly higher sequence similarity between *S. macrospora* and *P. nodorum* proteins from the cluster compared to the overall sequence similarity between other proteins from these species, and (3) the phylogenetic positioning of two of the clustered proteins within the Dothideomycetes rather

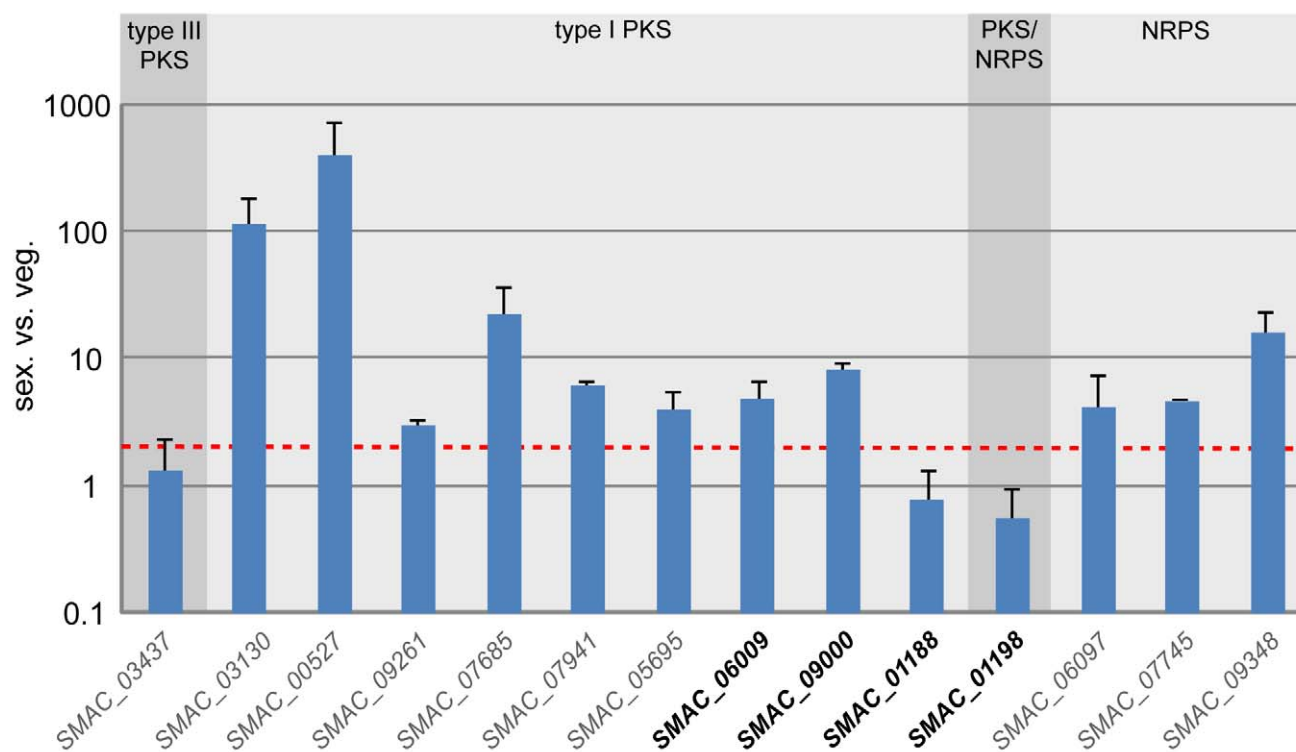


Figure 7. Expression of all predicted *pks* and *nrps* genes in *S. macrospora* during sexual development compared with vegetative growth. Gene names for which a *N. crassa* ortholog is present are given in gray, gene names where no *N. crassa* ortholog exists are given in bold black (see also Table S18). All expression data are the results of at least two independent experiments and were determined by quantitative real time PCR. Data for six of the genes (the first six type I *pks* genes, *SMAC_03130* to *SMAC_05695*) were taken from previous studies [36,78], expression of the other eight genes was determined in the course of this investigation. The type of encoded protein (type I PKS, type III PKS, PKS/NRPS hybrid, and NRPS) is indicated. The red line indicates two-fold upregulation.
doi:10.1371/journal.pgen.1000891.g007

than the Sordariomycetes are more consistent with HGT than with the hypothesis of gene duplication and subsequent gene loss even though the latter cannot be excluded [137]. Recent studies, made possible by the increasing number of fungal genome sequences, have indicated that HGT may be more common in fungi than previously thought, and that genes for secondary metabolism are especially prone to HGT [138–141]. Even though in many cases “non-canonic” phylogenetic tree topologies can be explained by a combination of duplication, diversification, and differential gene loss [138,142], that still leaves a number of cases where a HGT model best fits the observed data [140,141,143,144]. HGT may be one way for fungi to increase their biochemical repertoire, thereby increasing their ability to adapt to new ecological niches [137].

In the case of the *S. macrospora* cluster presented here, it is interesting to note that it contains two putative *pks* genes (*SMAC_01188* and *SMAC_01198*), one of which (*SMAC_01198*) has acquired 16 frame shifts/stop codons that interrupt the open reading frame whereas the other *pks* gene *SMAC_01188* as well as the additional ten genes that comprise the putative polyketide biosynthesis cluster represent functional genes. For seven of the twelve genes from the cluster (*SMAC_01188* to *SMAC_01191*, *SMAC_01194*, *SMAC_01196* and *SMAC_01198*), transcriptional expression was verified by cDNA sequencing, and spliced cDNAs were obtained for all of the genes including *SMAC_01198* which is unlikely to yield a functional protein due to the frameshifts (data not shown). Thus, this cluster might represent a case of an evolutionary recent acquisition that was introduced into the *S. macrospora* genome since its divergence from the last common

ancestor with *N. crassa*. While part of the cluster appears to be retained and under purifying selection in *S. macrospora*, the gene *SMAC_01198* has drifted and accumulated frameshift/nonsense mutations, even though it is still transcribed. Further analyses are necessary to determine the function of this putative polyketide biosynthesis cluster in *S. macrospora*.

Conclusions

Due to their high throughput and low costs, next-generation sequencing techniques have greatly changed the way large-scale sequencing projects are done. This includes e.g. re-sequencing of existing genomes for the discovery of variations, “RNA-sequencing” for transcriptome analysis, or “ChIP-Seq” for the genome-wide analysis of DNA-protein interactions [8]. Until recently, *de novo* genome assembly from next-generation sequences has been restricted to prokaryotic genomes [10,11]. This is due to the fact that eukaryotic genomes are larger and often contain high amounts of repetitive sequences that cannot be assembled from read lengths that are smaller than the length of the repeats. With the recent release of the Giant Panda genome [13] it has become obvious that even more complex eukaryotic genomes can be sequenced and assembled from short reads. Here, we present a high-quality draft of the *S. macrospora* genome, assembled solely from next-generation sequences, showing that *de novo* assembly from Solexa paired-end reads in combination with 454 sequence reads is feasible, cost-effective and fast, at least for compact eukaryotic genomes with few repetitive sequences.

Additionally, the *S. macrospora* genome revealed several features that are of interest with respect to fungal evolution, namely its

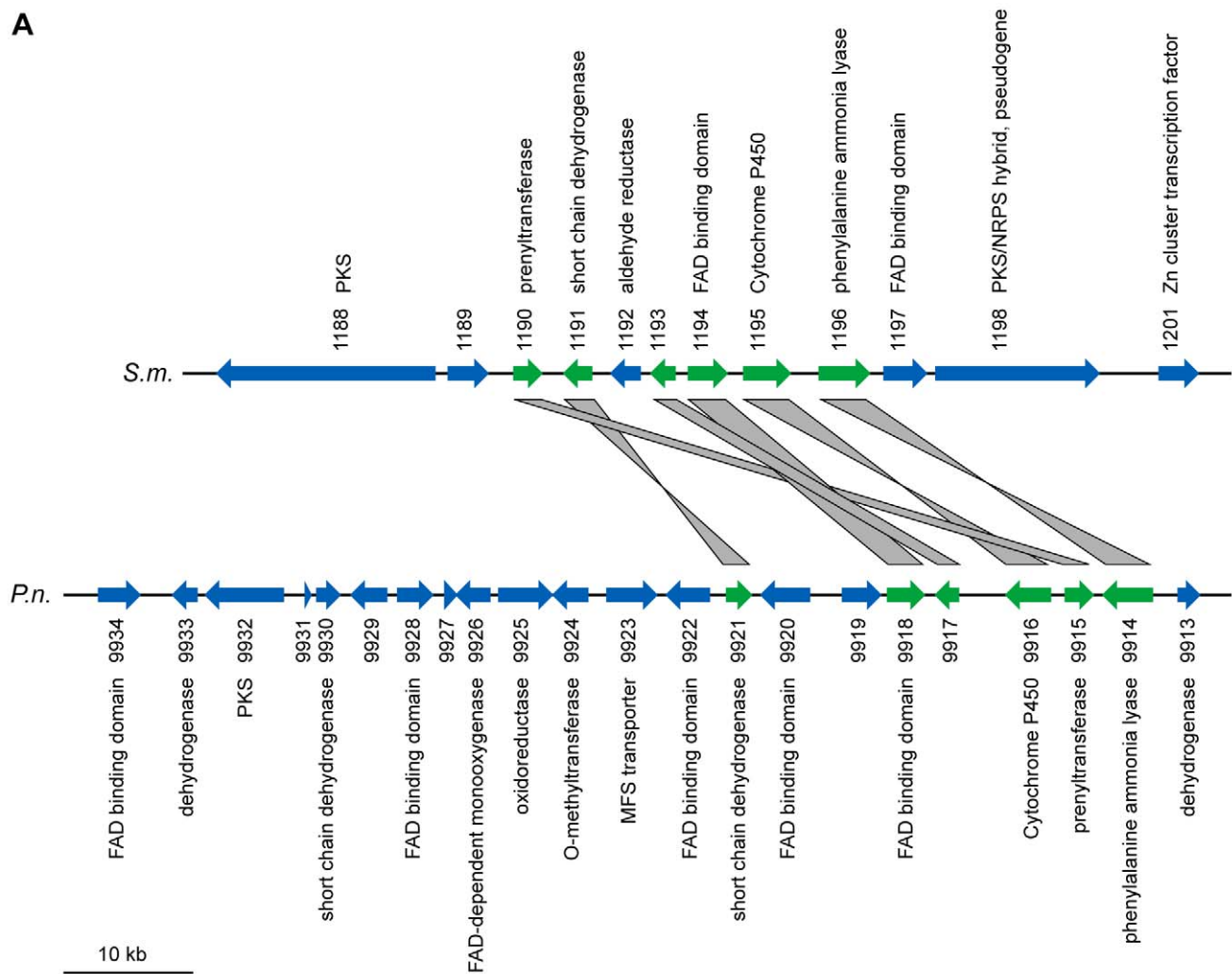
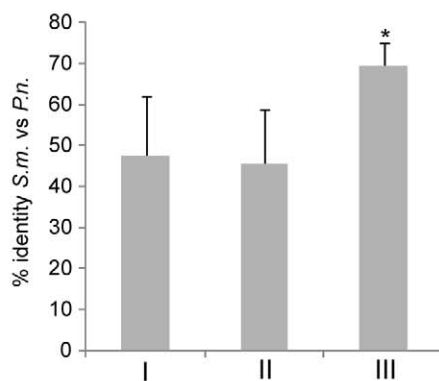
A**B**

Figure 8. A partly orthologous polyketide biosynthesis cluster in *S. macrospora* and *Phaeosphaeria nodorum*. (A) Comparison of partly orthologous polyketide biosynthesis clusters from *S. macrospora* (scaffold_17, *S.m.*) and *P. nodorum* (supercontig 16, *P.n.*, data for *P. nodorum* are from the *Stagonospora nodorum* database at http://www.broadinstitute.org/annotation/genome/stagonospora_nodorum/Home.html [136]). The six genes for which an ortholog is present in both clusters are shown in green, orthology is indicated by gray bars between the genes. Genes for which no orthologs are present in both clusters are given in blue. (B) Percent identity from BLASTP analysis (e-value $\leq 10^{-5}$) from a comparison of *S. macrospora* proteins versus *P. nodorum* proteins. Mean values of percent protein identity were calculated for (I) all proteins with a significant hit (e-value $\leq 10^{-5}$, 7424 proteins), (II) all proteins that contain a Pfam domain from one of the five Pfam domain families that are represented within the orthologous proteins from the cluster (137 proteins, the domains are adh_short, FAD_binding_3, p450, PAL, and UbiA, Table S8), (III) the orthologous proteins from the cluster (six proteins, indicated in green in A). The mean percent sequence identity for the orthologous proteins from the cluster is significantly higher ($p=0.001$) than either of the other two mean sequence identity values as indicated by an asterisk. doi:10.1371/journal.pgen.1000891.g008

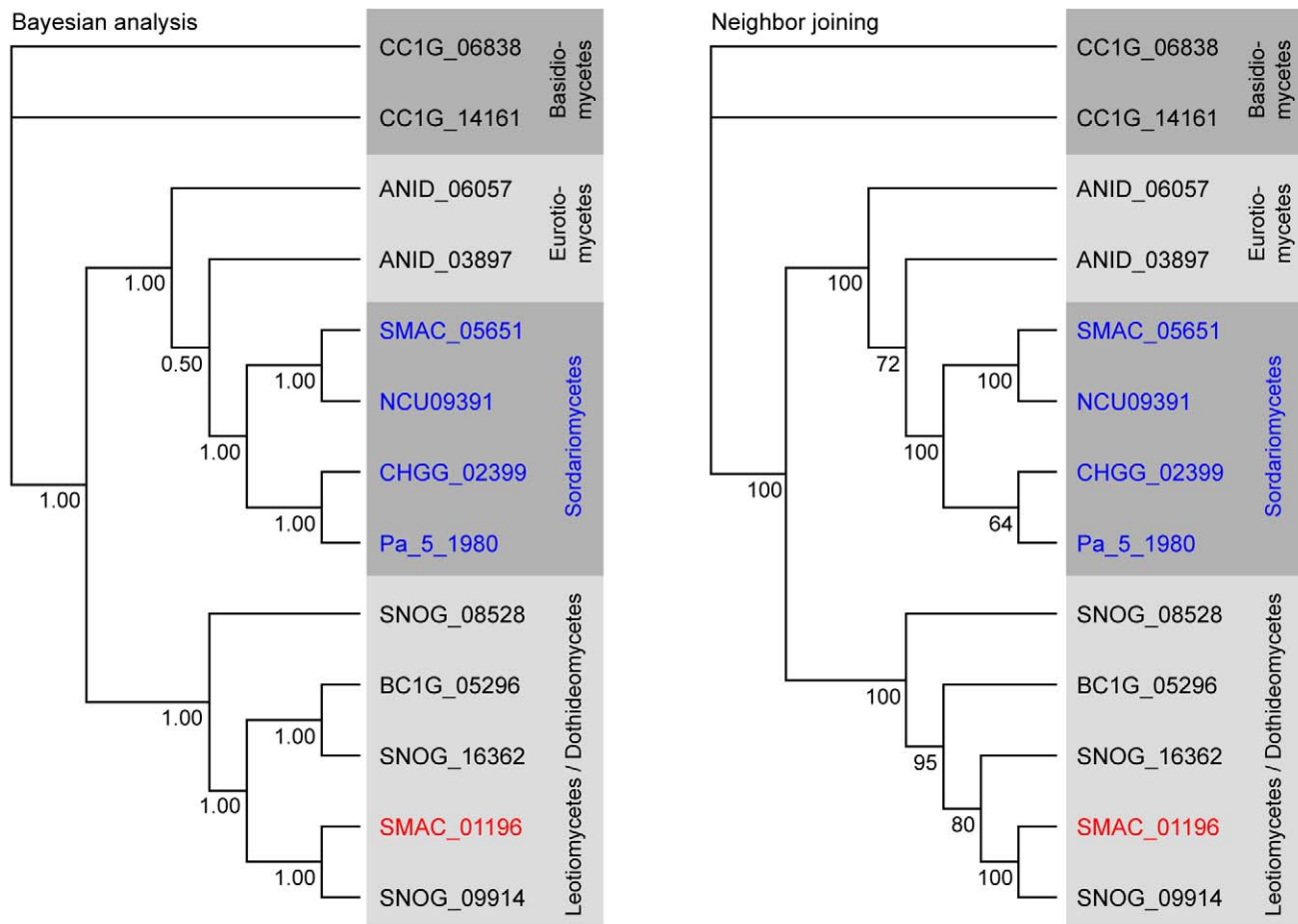


Figure 9. Phylogenetic analysis of the predicted phenylalanine ammonia lyase (PAL) proteins from eight fungi. Numbers at branches indicate bootstrap support (10,000 bootstrap replications) in % for the neighbor joining tree, and clade credibilities for the Bayesian tree. Classes given on the right correspond to the taxonomy used by Liu and Hall [171], and in the NCBI Entrez Taxonomy Database (<http://www.ncbi.nlm.nih.gov/entrez/query.fcgi?db=Taxonomy>). Sordariomycete proteins are given in blue with the exception of the *S. macrospora* protein SMAC_01196 that clusters with the Leotiomycete/Dothideomycete group and is given in red. Sequences for *P. anserina* were obtained from the *Podospira anserina* genome project (<http://podospira.igmors.u-psud.fr/index.html>) and for all other fungi from the Fungal Genome Initiative of the Broad Institute at (<http://www.broad.mit.edu/annotation/fungi/fgi/index.html>). AN: *Aspergillus nidulans*, BC: *Botrytis cinerea*, CC: *Coprinus cinereus* (outgroup), CH: *Chaetomium globosum*, NC: *Neurospora crassa*, SM: *Sordaria macrospora*, PA: *Podospira anserina*, SN: *Stagonospora nodorum* (*Phaeosphaeria nodorum*). doi:10.1371/journal.pgen.1000891.g009

complement of *het* genes as well as polyketide biosynthesis genes. In the case of the closely linked *het-c* and *pin-c* genes, it was found that *S. macrospora* contains additional copies that might have arisen from inversion/duplication events. In other fungi, the presence of non-identical *het* alleles within one cytoplasm leads to HI, which in its extreme results in cell death [109,115]. In contrast, *S. macrospora* is able to cope with this situation as no obvious HI phenotypes are observed in this fungus. However, we suggest that the aconidial phenotype of *S. macrospora* may be the result of “cryptic HI” caused by the presence of incompatible *het* genes within a single genome. Furthermore, analysis of a second *het* gene locus shows how the analysis of closely related genome sequences can help to pinpoint evolutionary events, in this case the occurrence of an inversion after separation of *Sordaria* and *Neurospora* but before speciation of *N. crassa* and *N. tetrasperma*. The analysis of predicted polyketide biosynthesis genes showed that *S. macrospora* contains more *pks* genes than its close relative *N. crassa*, and therefore probably has a wider biochemical repertoire available. One putative polyketide biosynthesis cluster might have been acquired through HGT, and this fits with previous results that show that HGT is probably

rather widespread in fungi both for the transfer of single genes, clustered genes like polyketide biosynthesis genes, or even larger stretches of DNA up to whole chromosomes as was found in the phytopathogenic fungus *Nectria haematococca* [139–141,143,144]. These findings support the theory that HGT plays a role in fungal evolution and might be a source of genetic variation that allows fungi to adapt to different ecological niches [137].

Materials and Methods

Strains and culture conditions

The sequenced reference strain is *Sordaria macrospora* k-hell from the strain collection of the Department of General and Molecular Botany at the Ruhr-Universität Bochum. The strain was grown on cornmeal medium as previously described [38].

DNA preparation for sequencing

Genomic DNA from *S. macrospora* was prepared by following a modified previously published method [145]. Mycelium was frozen in liquid nitrogen, pulverized, and incubated in equal

volumes of lysis buffer (0.2 M sodium borate, 30 mM EDTA, 1% SDS, pH 9.0) and phenol at 60°C for 5 min. After centrifugation, the supernatant was treated with RNase, and afterwards with an equal volume phenol/chloroform (1:1). After centrifugation, genomic DNA was purified from the supernatant by cesium chloride density gradient centrifugation.

Illumina/Solexa sequencing by synthesis

To construct libraries of two different insert sizes, 5 µg DNA each were sonicated with a Branson sonicator. Sonicated DNA was separated through 2% NuSieve agarose gels and fragments of ~300 and ~500 bp were purified. After generation of blunt-end fragments, A-overhangs were added, adaptors ligated, and the fragments were PCR amplified [146]. The resulting libraries were sequenced on an Illumina Genome Analyzer with a paired-end module generating reads of 36 bases. Four lanes from the 300 bp library and three lanes from the 500 bp library resulted in 3.4 Gb of sequence data (Table 1, Figure S1).

Roche/454 pyrosequencing

Roche/454 sequencing was performed with 50 µg genomic DNA at Eurofins MWG GmbH (Ebersberg, Germany). This resulted in 415 Mb of sequence data with an average read length of 367 bp (Table 1). The 454 raw data were extracted from the sff file and converted to a fasta file using sff_extract.py (written by Jose Blanca and Bastien Chevreux, http://bioinf.comav.upv.es/sff_extract/index.html).

Assembly

Assembly of the Solexa reads only as well as the combined Solexa and 454 reads was carried out with the Velvet assembler [42]. A description of the parameters used with Velvet can be found in Text S1 and Figure S1. An assembly of only the 454 data with the Celera Assembler 5.3 was performed by Eurofins MWG GmbH (Ebersberg, Germany). Comparison of the *S. macrospora* genome with the *N. crassa* genome [43] was done with BLAST [147] and visualized with Combo [148]. Comparative assembly of the *S. macrospora* genome along the genome sequences of *N. crassa*, *N. discreta* (<http://genome.jgi-psf.org/Neudi1/Neudi1.home.html>) and *N. tetrasperma* (<http://genome.jgi-psf.org/Neute1/Neute1.home.html>) genomes was done with Mercator [44]. Assembly of the mitochondrial genome and the rDNA unit was done with CodonCode Aligner version 3.0.3 (<http://www.codoncode.com/aligner/>), details can be found in Text S1 and Figure S3.

Annotation

Gene models were predicted independently with the *ab initio* predictors AUGUSTUS, GeneMark+ES, SNAP, and the evidence-based predictor Genewise [149–153]. The *ab initio* SNAP and AUGUSTUS parameters were trained on all *N. crassa* gene models while GeneMark performs an iterative self-training procedure. The Genewise predictions were generated from *N. crassa* proteins aligned to the genome by first aligning the proteins with TBLASTN, choosing the *S. macrospora* locus with only the best alignment for each protein and then refining the alignment and splice-sites with Genewise. The processing of outputs from these tools was completed with custom scripts utilizing tools from the BioPerl toolkit [154]. The resulting GFF annotation from each of the prediction programs was used as input to Evigan, a program that integrates the four sources of gene evidence [45].

For each of the predicted proteins, the protein with the highest sequence identity in GenBank was determined using BLASTP [147] (Table S2). Additionally, putative domains were predicted

with the HMMER (version 2.3.2) program hmmpfam using the hidden Markov models from the pfam database [49,50] and with the InterProScan function from Blast2GO [51,52]. The resulting data can be found in Table S8. Putative localization of the predicted proteins was determined with WoLF PSORT [155], putative signal peptides and signal anchors were predicted with SignalP 3.0 [156], and transmembrane domains with HMMTOP [157] and TMHMM [158] (Table S2, Text S2). tRNAs were predicted using a combination of Infernal 1.0, tRNAscan-SE, and TFAM 1.0 [159–161]. Orthologous groups of genes among the five fungal species *S. macrospora*, *N. crassa* [43], *N. discreta* (<http://genome.jgi-psf.org/Neudi1/Neudi1.home.html>), *P. anserina* [102], and *C. globosum* (http://www.broadinstitute.org/annotation/genome/chaetomium_globosum), *Chaetomium globosum* Sequencing Project, Broad Institute of Harvard and MIT <http://www.broad.mit.edu>) were identified with OrthoMCL [53]. Searches for transposons and repeat elements were done with BLAST [147] and by searches in Repbase (<http://www.girinst.org/>) [59].

For comparison of different genomic regions (CDSs, introns and upstream regions) from *S. macrospora*, *N. crassa*, *N. discreta* and *N. tetrasperma*, a Mercator alignment [44] of the genome sequences was performed and the parts of the alignment corresponding to the genomic regions were used to compute pairwise identities and evolutionary distances. Only those upstream regions were used that do not overlap with a protein coding region, and each region was used only once even if it is upstream of two divergently transcribed genes to avoid double-counting.

Accession numbers

The sequence and annotation data are available under the accession numbers CABT01000001–CABT01004783. The sequence reads that were used for the assembly of the *S. macrospora* genome were submitted to the NCBI sequence read archive (accession number SRA010462).

RNA preparation and expression analysis

For comparison of vegetative growth versus sexual development, growth and harvesting of *S. macrospora* and *N. crassa*, RNA preparation, reverse transcription and quantitative real time PCR were as described previously [19,162].

Phylogenetic analysis

Multiple alignments were created in CLUSTALX [163] and trimmed with Jalview [164], and the same alignment was used for analysis by distance-matrix (DM), maximum parsimony (MP) or Bayesian methods. Phylogenetic analyses were made with PAUP version 4.0b10 for Windows (D.L. Swofford, distributed by Sinauer Associates, copyright 2001 Smithsonian Institution) for DM and MP analyses, and with MrBayes [165,166]. DM and MP analyses were performed as described using 10,000 bootstrap replicates, Bayesian analysis was performed with at least 250,000 generations [167]. Consensus trees were graphically displayed with TREEVIEW or Dendroscope [168,169].

Supporting Information

Figure S1 Next-generation sequencing of the *S. macrospora* genome. (A) Summary of the Illumina/Solexa and 454 sequences that were obtained. (B) Maximum contig lengths (N max) and N50 values for assemblies with different k-values (hash length in Velvet) for the Illumina/Solexa data alone or in combination with the 454 data. The combined assembly with the highest N max and N50 value (k = 25) was used for further analyses. Found at: doi:10.1371/journal.pgen.1000891.s001 (0.40 MB TIF)

Figure S2 Assemblies with different coverage levels of short reads. Assemblies were done with Velvet 0.7.56 with $k = 25$. N50, maximum contig length (Nmax), the number of gaps that Velvet introduced within contigs and the total length of gaps within the assembly are given for different combinations of 454 coverage (x-axis), coverage from a 300 bp Solexa paired-end library ($25\times$ coverage in (A–D), $50\times$ coverage in (E–H), respectively), and coverage from a 500 bp Solexa paired-end library ($0\times$, $9\times$, $18\times$, and $27\times$ coverage as color-coded in the different panels). Addition of 454 reads has the most drastic effect on the number and length of gaps (note the logarithmic y-axis for these panels) whereas addition of paired-end reads influences mostly N50 and Nmax. A table with assembly information for additional coverage combinations can be found in Table S1.

Found at: doi:10.1371/journal.pgen.1000891.s002 (1.07 MB TIF)

Figure S3 The mitochondrial genome of *S. macrospora*. (A) Schematic map of the mitochondrial genome. Size 88,423 bp, scale in kb indicated on the inner circle. Blue: ribosomal RNAs, green: tRNAs, red: protein coding genes, orange on the inner circle: open reading frames within introns of protein coding genes. Note that all predicted genes are encoded on the same strand. (B, C) Comparative analysis of the mitochondrial DNA of *S. macrospora* with *N. crassa* (B) and *P. aserina* (C). Dot plots of BLASTN analysis that was done at <http://blast.ncbi.nlm.nih.gov/Blast.cgi> with an e-value cutoff of 10^{-20} .

Found at: doi:10.1371/journal.pgen.1000891.s003 (0.35 MB TIF)

Figure S4 Histograms of % pairwise identity between *S. macrospora* and *N. crassa* for different genomic regions. CDSs, introns, and regions upstream of CDSs (in 1 kb steps ranging from 1 to 4 kb) were used for comparison. Only those upstream regions were used that do not overlap with a protein coding region. Each region was used only once even if it is upstream of two divergently transcribed genes to avoid double-counting. Detailed information on the comparisons can be found in Table S5.

Found at: doi:10.1371/journal.pgen.1000891.s004 (0.65 MB TIF)

Figure S5 Phylogenetic analysis of orthogroups 49 (A) and 180 (B) and related orthogroups. With the exception of orthogroup 6050, which is split in two parts, all orthogroups that were found by OrthoMCL are supported by phylogenetic analysis. Most orthogroups contain one member each in *S. macrospora*, *N. crassa*, and *N. discreta*, but orthogroups 49 and 180 contain six and four members, respectively, from *S. macrospora*. Thus, both the OrthoMCL analysis as well as the phylogenetic trees constructed with maximum parsimony support the hypothesis that orthogroups 49 and 180 are part of larger gene families, but that in these branches of the gene families, recent gene duplication events occurred specifically in *S. macrospora*. Numbers at branches indicate bootstrap support (10,000 bootstrap replications) in % for maximum parsimony trees. SM: *S. macrospora*, NC: *N. crassa*, ND: *N. discreta*, CHG: *C. globosum*, PA: *P. aserina*.

Found at: doi:10.1371/journal.pgen.1000891.s005 (0.72 MB TIF)

Figure S6 Regions of high similarity within four fungal genomes. Each genome sequence was compared to itself with BLASTN with e-value $< 10^{-150}$. Dot plot visualization was done with Combo (Engels et al. 2006, Bioinformatics 22: 1782–1783). The *M. grisea* genome contains a high amount of repeated DNA (Dean et al. 2005, Nature 434 :980–986), and this is reflected in this comparison. The genomes of *N. crassa* (Galagan et al. 2003, Nature 422: 859–868) and *F. graminearum* (Cuomo et al. 2007, Science 317: 1400–1402) contain only few repeat regions. The intragenomic similarities within the *S. macrospora* genome range between those for *N. crassa* and *F. graminearum*.

Found at: doi:10.1371/journal.pgen.1000891.s006 (0.87 MB TIF)

Figure S7 Comparison of RIP indices in the *S. macrospora* and *N. crassa* genomes. (A) No evidence for large regions with RIP in the *S. macrospora* genome. The substrate ([CA+TG]/[AC+GT]; orange) and product (TpA/ApT; dark green) RIP indices were calculated for all unscaffolded contigs (nt 1 to 2,865,981), the mtDNA (nt 2,865,982 to 2,954,404) and random scaffolds (nt 2,954,405 to 5,000,000). The patterns for the remainder of the *S. macrospora* genome look similar to those shown here for the random scaffolds. We predicted that the unscaffolded contigs would be AT-rich and would show hallmarks of RIP. Instead, these contigs are GC-rich and show now evidence for RIP by this assay. The mtDNA (black arrow) has balanced AT and GC content, more resembling bacterial DNA and thus has a different pattern than *S. macrospora* nuclear DNA. (B) Evidence for RIP in *N. crassa* Linkage Group I. The first 5 Mb of LGI of *N. crassa* were analyzed as above. High values for the product RIP index (green), coupled with low values for the substrate RIP index (orange) reveal dispersed (blue arrows) and centromeric (red arrowhead) regions that have been subjected to RIP.

Found at: doi:10.1371/journal.pgen.1000891.s007 (0.57 MB TIF)

Figure S8 Perithecial neck phototropisms in response to unilateral light of different wavelengths. (A–C) Positive neck phototropisms in response to white light (A, fluence rate $3.4 \mu\text{M}/\text{m}^2\text{s}$), blue light (B, wavelength: 470 nm; fluence rate $6.3 \mu\text{M}/\text{m}^2\text{s}$), and green light (C, wavelength: 530 nm; fluence rate $3.4 \mu\text{M}/\text{m}^2\text{s}$). (D, E) No neck phototropisms under red light (D, wavelength: 680 nm; fluence rate $5.4 \mu\text{M}/\text{m}^2\text{s}$) or complete darkness (E). The arrows indicate the direction of neck tropisms.

Found at: doi:10.1371/journal.pgen.1000891.s008 (1.08 MB TIF)

Figure S9 Expression of *S. macrospora* genes that are orthologs of genes involved in conidiation in *N. crassa*. Transcript levels were compared between sexual development and vegetative growth. Expression data are the results of two independent experiments and were determined by quantitative real time PCR. The red dashed line indicates two-fold upregulation. In *N. crassa*, the corresponding orthologs are regulators of conidiation (*fluffy*, *csp-1*, *rco-1*, *rco-3*) or encode structural proteins (*cgg-2*) or enzymes (*al-1*) that are important for conidiospore morphology. All six *S. macrospora* orthologs are transcribed both during vegetative growth and sexual development, and several are upregulated during sexual development. The strongest upregulation is observed in the *cgg-2* ortholog *SMAC_00022*. In *N. crassa*, *cgg-2* encodes a hydrophobin that forms the hydrophobic coat (rodlet layer) of the conidial cell wall (Bell-Pedersen et al. 1992 Genes Dev 6: 2382–2394). Generally, fungal hydrophobins are expressed when hyphae encounter an air/water interface (Wösten 1991 Annu Rev Microbiol 2001. 55:625–646), and this might be the reason why the *S. macrospora* *cgg-2* ortholog is only weakly expressed in the submerged culture used to obtain vegetative mycelium but strongly upregulated under conditions for sexual development, i.e. during growth as a surface culture. The function of these genes in the aconidial *S. macrospora* is unknown. Several of the *N. crassa* orthologs have functions outside of conidiation, e.g. the putative transcriptional repressor *rco-1* (Yamashiro et al. 1996 Mol Cell Biol 16: 6218–6228) or the glucose transporter *rco-3* (Madi et al. 1997 Genetics 146: 499–508), but others like the transcription factor-encoding genes *fluffy* (Bailey and Ebbole 1998 Genetics 148: 1813–1820) and *csp-1* (Lambrechts et al. 2009 Genetics 181: 767–781) are specific to conidiation and their function in *S. macrospora* remains to be elucidated.

Found at: doi:10.1371/journal.pgen.1000891.s009 (0.21 MB TIF)

Figure S10 The *het-6/un-24* locus from *S. macrospora* is syntenic to the OR allele of *N. crassa*. (A) Region from *S. macrospora* scaffold 5 and *N. crassa* scaffold 8 containing *het-6* and *un-24* genes. Homologous genes are given in the same color. The two different allelic combinations of *het-6* and *un-24* in *N. crassa*, Oak Ridge (OR) and Panama (PA), are indicated. The *S. macrospora* gene order resembles that of the Oak Ridge strain. *SMAC_07776* contains three stop codons within the open reading frame (indicated by asterisks above the gene) and is therefore probably a pseudogene or it encodes a shorter HET-6. (B) Phylogenetic analysis of partial HET-6 and UN-24 proteins from *S. macrospora*, *N. crassa* (NC) and *N. tetrasperma* (NT). For *N. tetrasperma*, OR alleles were taken from strain P514, PA alleles from strain P2361 (Powell et al., Fungal Genet Biol 2007, 44: 896–904). The homologous *P. anserina* proteins were used as an outgroup to root the trees. Bootstrap values in % (10,000 bootstrap replicates) are given for maximum parsimony and neighbor joining trees above and below the branches, respectively. OR and PA alleles from the two different *Neurospora* species cluster together whereas *S. macrospora* is basal to the *Neurospora* proteins indicating that the Oak Ridge gene order is probably ancient and the Panama gene order has arisen from an inversion after separation of the genus *Neurospora* from the genus *Sordaria* and before speciation of *N. crassa* and *N. tetrasperma*.

Found at: doi:10.1371/journal.pgen.1000891.s010 (0.18 MB TIF)

Figure S11 Summary of all proteins in *S. macrospora* that are predicted to be PKSs or NRPSs.

Found at: doi:10.1371/journal.pgen.1000891.s011 (0.44 MB TIF)

Figure S12 Phylogenetic analysis of the UbiA prenyltransferase family proteins from 12 fungi. The *S. macrospora* protein SMAC_01190 clusters in a group of “outsider” proteins with not quite clear phylogenetic resolution (bootstrap support of only 60 % as indicated in a red circle), most likely due to gene family expansion in *Aspergillus*/*Neosartorya*/*Stagonospora*/*Botrytis*/*Sclerotinia*. However, as it clusters with SNOG_09915, this might indicate horizontal gene transfer. Numbers at branches indicate bootstrap support (10,000 bootstrap replications) in % for the neighbor joining tree. *Sordariales* proteins are given in blue with the exception of the *S. macrospora* protein SMAC_01190 that clusters with the Dothideomycete *Stagonospora nodorum* and is given in red. Sequences that belong to the protoheme farnesyl transferase group are shaded in dark gray, sequences that belong to the polyprenyl transferase group are shaded in light gray. Sequences for *P. anserina* were obtained from the *Podospora anserina* genome project (<http://podospora.igmors.u-psud.fr/index.html>) and for all other fungi from the Fungal Genome Initiative of the Broad Institute at (<http://www.broad.mit.edu/annotation/fungi/fgi/index.html>) or from our own data (*S. macrospora*). AN: *Aspergillus nidulans*, BC: *Botrytis cinerea*, CH: *Chaetomium globosum*, FG: *Fusarium graminearum*, MG: *Magnaporthe grisea*, NC: *Neurospora crassa*, NF: *Neosartorya fischeri*, PA: *Podospora anserina*, SM: *Sordaria macrospora*, SN: *Stagonospora nodorum* (*Phaeosphaeria nodorum*), SS: *Sclerotinia sclerotiorum*, Y: *Saccharomyces cerevisiae*.

Found at: doi:10.1371/journal.pgen.1000891.s012 (0.33 MB TIF)

Table S1 Assemblies with different coverage levels.

Found at: doi:10.1371/journal.pgen.1000891.s013 (0.19 MB PDF)

Table S2 Overview of predicted *S. macrospora* genes.

Found at: doi:10.1371/journal.pgen.1000891.s014 (7.09 MB XLS)

Table S3 Orthologs between *S. macrospora* and *N. crassa*.

Found at: doi:10.1371/journal.pgen.1000891.s015 (1.02 MB XLS)

Table S4 Orphan genes.

Found at: doi:10.1371/journal.pgen.1000891.s016 (0.37 MB XLS)

Table S5 Comparisons of different genomic regions.

Found at: doi:10.1371/journal.pgen.1000891.s017 (4.61 MB XLS)

Table S6 hmmpfam predictions.

Found at: doi:10.1371/journal.pgen.1000891.s018 (1.22 MB XLS)

Table S7 OrthoMCL family species count.

Found at: doi:10.1371/journal.pgen.1000891.s019 (1.18 MB XLS)

Table S8 OrthoMCL orthogroups.

Found at: doi:10.1371/journal.pgen.1000891.s020 (1.66 MB XLS)

Table S9 Genome integrity genes.

Found at: doi:10.1371/journal.pgen.1000891.s021 (0.35 MB XLS)

Table S10 Homologs to genes involved in light signaling and regulation.

Found at: doi:10.1371/journal.pgen.1000891.s022 (0.05 MB PDF)

Table S11 Homologs to genes involved in senescence.

Found at: doi:10.1371/journal.pgen.1000891.s023 (0.07 MB PDF)

Table S12 Genes with putative functions in calcium signaling.

Found at: doi:10.1371/journal.pgen.1000891.s024 (0.07 MB PDF)

Table S13 Genes with putative functions as motor proteins.

Found at: doi:10.1371/journal.pgen.1000891.s025 (0.07 MB PDF)

Table S14 Genes with putative functions in MAP kinase and phospholipid signaling.

Found at: doi:10.1371/journal.pgen.1000891.s026 (0.09 MB PDF)

Table S15 Known and putative meiosis genes.

Found at: doi:10.1371/journal.pgen.1000891.s027 (0.09 MB XLS)

Table S16 *S. macrospora* homologs of conidiation-related genes from different ascomycetes.

Found at: doi:10.1371/journal.pgen.1000891.s028 (0.07 MB PDF)

Table S17 *S. macrospora* homologs of genes involved in heterokaryon incompatibility from different ascomycetes.

Found at: doi:10.1371/journal.pgen.1000891.s029 (0.06 MB PDF)

Table S18 Predicted polyketide synthases (PKS), non-ribosomal peptide synthases (NRPS), and fatty acid synthases (FAS).

Found at: doi:10.1371/journal.pgen.1000891.s030 (0.06 MB PDF)

Table S19 A putative polyketide biosynthesis cluster that is partly conserved in *S. macrospora* and *Phaeosphaeria nodorum*.

Found at: doi:10.1371/journal.pgen.1000891.s031 (0.06 MB PDF)

Text S1 Parameters used for the assembly of the *S. macrospora* genome.

Found at: doi:10.1371/journal.pgen.1000891.s032 (0.05 MB PDF)

Text S2 Predicted subcellular localizations, signal peptides, and transmembrane domains for the *S. macrospora* proteins.

Found at: doi:10.1371/journal.pgen.1000891.s033 (0.08 MB PDF)

Acknowledgments

We thank Mark Dasenko, Steve Drake, Chris Sullivan, and Scott Givan at the OSU CGRB core facility for Illumina sequencing. We would like to thank Ingeborg Godehardt and Swenja Ellßel (Ruhr-Universität Bochum) for

excellent technical assistance; Sebastian Veit, Tim Dahlmann, and Daniel Schindler (Ruhr-Universität Bochum) for help with some of the annotation; Kerstin Howe and Ulrike Böhme (Wellcome Trust Sanger Institute) for helpful hints about genome annotation software; and John Taylor (UC Berkeley), Louise Glass (UC Berkeley), Don Natvig (University of New Mexico), David Jacobson (UC Berkeley), and the JGI (DOE Joint Genome Institute) for sharing *Neurospora discreta* and *Neurospora tetrasperma* data prior to publication.

Author Contributions

Conceived and designed the experiments: MN UK MF. Performed the experiments: MN JES MC JK FK KMS MF. Analyzed the data: MN JES

References

- Hawksworth DL (2001) The magnitude of fungal diversity: the 1.5 million species estimate revisited. *Mycol Res* 105: 1422–1432.
- Stajich JE, Berbee ML, Blackwell M, Hibbett DS, James TY, et al. (2009) The fungi. *Curr Biol* 19: R840–R845.
- Buckley M (2008) The fungal kingdom - diverse and essential roles in earth's ecosystem. Washington DC: American Academy of Microbiology.
- Smith SE, Read DJ (2000) Mycorrhizal symbiosis. London, San Diego: Academic Press.
- Archer DB, Connerton IF, MacKenzie DA (2008) Filamentous fungi for production of food additives and processing aids. *Adv Biochem Eng Biotechnol* 111: 99–147.
- Hoffmeister D, Keller NP (2007) Natural products of filamentous fungi: enzymes, genes, and their regulation. *Nat Prod Rep* 24: 393–416.
- Goffeau A, Barrell BG, Bussey H, Davis RW, Dujon B, et al. (1996) Life with 6000 genes. *Science* 274: 546–567.
- Shendure J, Li H (2008) Next-generation DNA sequencing. *Nature Biotechnol* 26: 1135–1145.
- Whiteford N, Haslam N, Weber G, Prügel-Bennett A, Essex JW, et al. (2005) An analysis of the feasibility of short read sequencing. *Nucl Acids Res* 33: e171.
- Margulies M, Egholm M, Altman WE, Attiya S, Bader JS, et al. (2005) Genome sequencing in microfabricated high-density picolitre reactors. *Nature* 437: 376–380.
- Reinhardt JA, Baltrus DA, Nishimura MT, Jeck WR, Jones CD, et al. (2009) *De novo* assembly using low-coverage short read sequence data from the rice pathogen *Pseudomonas syringae* pv. *oryzae*. *Genome Res* 19: 294–305.
- DiGiustini S, Liao N, Platt D, Robertson G, Seidel M, et al. (2009) *De novo* genome sequence assembly of a filamentous fungus using Sanger, 454 and Illumina sequence data. *Genome Biol* 10: R94.
- Li R, Fan W, Tian G, Zhu H, He L, et al. (2009) The sequence and *de novo* assembly of the giant panda genome. *Nature advance online publication*: doi:10.1038/nature08696.
- Kück U, Pöggeler S, Nowrousian M, Nolting N, Engh I (2009) *Sordaria macrospora*, a model system for fungal development. In: Anke T, Weber D, eds. *The Mycota XV, Physiology and Genetics*. 1st ed. Berlin, Heidelberg: Springer. pp 17–39.
- Zickler D (2005) Meiosis in mycelial fungi. In: Kües U, Fischer R, eds. *The Mycota I Growth, differentiation and sexuality*. Berlin, Heidelberg: Springer. pp 415–438.
- Zickler D (2006) From early homologue recognition to synaptonemal complex formation. *Chromosoma* 115: 158–174.
- Pöggeler S, Nowrousian M, Kück U (2006) Fruiting-body development in ascomycetes. In: Kües U, Fischer R, eds. *The Mycota I*. Berlin, Heidelberg: Springer. pp 325–355.
- Esser K, Straub J (1958) Genetische Untersuchungen an *Sordaria macrospora* Auerw., Kompensation und Induktion bei genbedingten Entwicklungsdefekten. *Z Vererbungsl* 98: 729–746.
- Nowrousian M, Ringelberg C, Dunlap JC, Loros JJ, Kück U (2005) Cross-species microarray hybridization to identify developmentally regulated genes in the filamentous fungus *Sordaria macrospora*. *Mol Genet Genomics* 273: 137–149.
- Pöggeler S, Kück U (2006) Highly efficient generation of signal transduction knockout mutants using a fungal strain deficient in the mammalian *ku70* ortholog. *Gene* 378: 1–10.
- Pöggeler S, Masloff S, Hoff B, Mayrhofer S, Kück U (2003) Versatile EGFP reporter plasmids for cellular localization of recombinant gene products in filamentous fungi. *Curr Genet* 43: 54–61.
- Pöggeler S, Nowrousian M, Jacobsen S, Kück U (1997) An efficient procedure to isolate fungal genes from an indexed cosmid library. *J Microbiol Meth* 29: 49–61.
- Rech C, Engh I, Kück U (2007) Detection of hyphal fusion in filamentous fungi using differently fluorescence-labeled histones. *Curr Genet* 52: 259–266.
- Walz M, Kück U (1995) Transformation of *Sordaria macrospora* to hygromycin B resistance: characterization of transformants by electrophoretic karyotyping and tetrad analysis. *Curr Genet* 29: 88–95.
- Engh I, Würtz C, Witzel-Schlömp K, Zhang HY, Hoff B, et al. (2007) The VW domain protein PRO40 is required for fungal fertility and associates with Woronin bodies.
- IE EE KH JK FK BK HCK HDO SP NDR SS KMS DZ MF. Contributed reagents/materials/analysis tools: MN JES UK MF. Wrote the paper: MN JES NDR UK MF. Performed de novo assembly: MN. Performed expression and phylogenetic analyses: MN. Performed scaffolding of contigs, gene predictions, comparison of different genomic regions, and OrthoMCL analysis: JES. Performed photobiology analysis: MC KH NR. Performed Illumina/Solexa sequencing: MF. Performed manual annotation: MN IE EE JK FK BK HCK HDO SP SS KMS DZ MF.
- Masloff S, Pöggeler S, Kück U (1999) The *pro1+* gene from *Sordaria macrospora* encodes a C₆ zinc finger transcription factor required for fruiting body development. *Genetics* 152: 191–199.
- Nowrousian M, Frank S, Koers S, Strauch P, Weitner T, et al. (2007) The novel ER membrane protein PRO41 is essential for sexual development in the filamentous fungus *Sordaria macrospora*. *Mol Microbiol* 64: 923–937.
- Pöggeler S, Kück U (2004) A WD40 repeat protein regulates fungal cell differentiation and can be replaced functionally by the mammalian homologue striatin. *Eukaryot Cell* 3: 232–240.
- Storlazzi A, Tessé S, Gargano S, James F, Kleckner N, et al. (2003) Meiotic double-strand breaks at the interface of chromosome movement, chromosome remodeling, and reductional division. *Genes Dev* 17: 2675–2687.
- Storlazzi A, Tesse S, Ruprich-Robert G, Gargano S, Pöggeler S, et al. (2008) Coupling meiotic chromosome axis integrity to recombination. *Genes Dev* 22: 796–809.
- van Heemst D, James F, Pöggeler S, Bertaux-Lecellier V, Zickler D (1999) Spo76p is a conserved chromosome morphogenesis protein that links the mitotic and meiotic programs. *Cell* 98: 261–271.
- Nowrousian M, Masloff S, Pöggeler S, Kück U (1999) Cell differentiation during sexual development of the fungus *Sordaria macrospora* requires ATP citrate lyase activity. *Mol Cell Biol* 19: 450–460.
- McClintock B (1945) *Neurospora*. I. Preliminary observations of the chromosomes of *Neurospora crassa*. *Am J Bot* 32: 671–678.
- Orbach M, Vollrath D, Davis RW, Yanofsky C (1988) An electrophoretic karyotype of *Neurospora crassa*. *Mol Cell Biol* 8: 1469–1473.
- Pöggeler S, Masloff S, Jacobsen S, Kück U (2000) Karyotype polymorphism correlates with intraspecific infertility in the homothallic ascomycete *Sordaria macrospora*. *J Evol Biol* 13: 281–289.
- Nowrousian M (2009) A novel polyketide biosynthesis gene cluster is involved in fruiting body morphogenesis in the filamentous fungi *Sordaria macrospora* and *Neurospora crassa*. *Curr Genet* 55: 185–198.
- Nowrousian M, Würtz C, Pöggeler S, Kück U (2004) Comparative sequence analysis of *Sordaria macrospora* and *Neurospora crassa* as a means to improve genome annotation. *Fungal Genet Biol* 41: 285–292.
- Esser K (1982) *Cryptogams - Cyanobacteria, Algae, Fungi, Lichens*. London: Cambridge University Press.
- Perkins DD (1992) *Neurospora: the organism behind the molecular revolution*. *Genetics* 130: 687–701.
- Jacobson DJ, Dettman JR, Adams RI, Boels C, Sultana S, et al. (2006) New findings of *Neurospora* in Europe and comparisons of diversity in temperate climates on continental scales. *Mycologia* 98: 550–559.
- Jacobson DJ, Powell AJ, Dettman JR, Saenz GS, Barton MM, et al. (2004) *Neurospora* in temperate forests of western North America. *Mycologia* 96: 66–74.
- Zerbino DR, Birney E (2008) Velvet: Algorithms for de novo short read assembly using de Bruijn graphs. *Genome Res* 18: 821–829.
- Galagan JE, Calvo SE, Borkovich KA, Selker EU, Read ND, et al. (2003) The genome sequence of the filamentous fungus *Neurospora crassa*. *Nature* 422: 859–868.
- Dewey CN (2007) Aligning multiple whole genomes with Mercator and MAVID. In: Bergman NH, ed. *Comparative genomics*. Totowa: Humana Press.
- Liu Q, Mackey AJ, Roos DS, Pereira FCN (2008) Evigan: a hidden variable model for integrating gene evidence for eukaryotic gene predictions. *Bioinformatics* 24: 597–605.
- Branscomb E, Predki P (2002) On the high value of low standards. *J Bacteriol* 194: 6406–6409.
- Fraser CM, Eisen JA, Nelson KE, Paulsen IT, Salzberg SL (2002) The value of complete microbial genome sequencing (you get what you pay for). *J Bacteriol* 184: 6403–6405.
- Kasuga T, Mannhaupt G, Glass NL (2009) Relationship between phylogenetic distribution and genomic features in *Neurospora crassa*. *PLOS ONE* 4: e5286. doi:10.1371/journal.pone.0005286.
- Eddy SR (1998) Profile Hidden Markov Models. *Bioinformatics* 14: 755–763.
- Finn RD, Tate J, Misty J, Coghill PC, Sammut SJ, et al. (2008) The Pfam protein families database. *Nucl Acids Res* 36: D281–288.

51. Conesa A, Gotz S, Garcia-Gomez JM, Terol J, Talon M, et al. (2005) Blast2GO: a universal tool for annotation, visualization and analysis in functional genomics research. *Bioinformatics* 21: 3674–3676.
52. Zdobnov EM, Apweiler R (2001) InterProScan - an integration platform for the signature-recognition methods in InterPro. *Bioinformatics* 17: 847–848.
53. Li L, Stoeckert CII, Roos DS (2003) OrthoMCL: Identification of ortholog groups for eukaryotic genomes. *Genome Res* 13: 2178–2189.
54. Jurka J (1998) Repeats in genomic DNA: mining and meaning. *Curr Opin Struct Biol* 8: 333–337.
55. Schnable PS, Ware D, Fulton RS, Stein JC, Wei F, et al. (2009) The B73 maize genome: complexity, diversity, and dynamics. *Science* 326: 1112–1115.
56. Lynch M (2007) The origins of genome architecture. SunderlandMA: Sinauer Assoc. Inc.
57. Kempken F, Kück U (1998) Transposons in filamentous fungi - facts and perspectives. *Bioessays* 20: 652–659.
58. Braumann I, van den Berg M, Kempken F (2007) Transposons in biotechnologically relevant strains of *Aspergillus niger* and *Penicillium chrysogenum*. *Fungal Genet Biol* 44: 1399–1414.
59. Kapitonov VV, Jurka J (2008) A universal classification of eukaryotic transposable elements in Repbase. *Nat Rev Genet* 9: 411–412.
60. Kinsey J, Helber J (1989) Isolation of a transposable element from *Neurospora crassa*. *Proc Nat Acad Sci USA* 86: 1929–1933.
61. Kempken F, Windhofer F (2001) The *hAT* family: a versatile transposon group common to plants, fungi, animals, and man. *Chromosoma* 110: 1–9.
62. Daboussi MJ, Langin t, Brygoo Y (1992) *FotI*, a new family of fungal transposable elements. *Mol Gen Genet* 232: 12–16.
63. Cuomo CA, Guldener U, Xu JR, Trail F, Turgeon BG, et al. (2007) The *Fusarium graminearum* genome reveals a link between localized polymorphism and pathogen specialization. *Science* 317: 1400–1402.
64. Dean RA, Talbot NJ, Ebbole DJ, Farman ML, Mitchell TK, et al. (2005) The genome sequence of the rice blast fungus *Magnaporthe grisea*. *Nature* 434: 980–986.
65. Braumann I, van den Berg M, Kempken F (2008) Strain-specific retro-transposon-mediated recombination in a commercially used *Aspergillus niger* strain. *Mol Genet Genomics* 280: 319–325.
66. Rasmussen JP, Taylor AH, Ma IJ, Purcell S, Kempken F, et al. (2004) *Guest*, a transposable element belonging to the Tc1/mariner superfamily is an ancient invader of *Neurospora* genomes. *Fungal Genet Biol* 41: 52–61.
67. Graia F, Lespinet O, Rimbault B, Dequard-Chablat M, Coppin E, et al. (2001) Genome quality control: RIP (repeat-induced point mutation) comes to *Podospora*. *Mol Microbiol* 40: 586–595.
68. Hamann A, Feller F, Osiewacz HD (2000) The degenerate DNA transposon *Pat* and repeat-induced point mutation (RIP) in *Podospora anserina*. *Mol Gen Genet* 263: 1061–1069.
69. Ikeda K, Nakayashiki H, Kataoka T, Tamba H, Hashimoto Y, et al. (2002) Repeat-induced point mutation (RIP) in *Magnaporthe grisea*: implications for its sexual cycle in the natural field context. *Mol Microbiol* 45: 1355–1364.
70. Idnurm A, Howlett BJ (2003) Analysis of loss of pathogenicity mutants reveals that repeat-induced point mutations can occur in the Dothideomycete *Leptosphaeria maculans*. *Fungal Genet Biol* 39: 31–37.
71. Galagan JE, Selker EU (2004) RIP: the evolutionary cost of genome defense. *Trends Genet* 20: 417–423.
72. Margolin BS, Garrett-Engle PW, Stevens JN, Fritz DY, Garrett-Engle C, et al. (1998) A methylated *Neurospora* 5S rRNA pseudogene contains a transposable element inactivated by repeat-induced point mutation. *Genetics* 149: 1787–1797.
73. Freitag M, Williams RL, Kothe GO, Selker EU (2002) A cytosine methyltransferase homologue is essential for repeat-induced point mutation in *Neurospora crassa*. *Proc Nat Acad Sci USA* 99: 8802–8807.
74. Malagnac F, Wendel B, Goyon C, Faugeron G, Zickler D, et al. (1997) A gene essential for de novo methylation and development in *Ascomobolus* reveals a novel type of eukaryotic DNA methyltransferase structure. *Cell* 91: 281–290.
75. Lee DW, Freitag M, Selker EU, Aramayo R (2008) A cytosine methyltransferase homologue is essential for sexual development in *Aspergillus nidulans*. *PLoS ONE* 3: e2531. doi:10.1371/journal.pone.0002531.
76. Fulci V, Macino G (2007) Quelling: post-transcriptional gene silencing guided by small RNAs in *Neurospora crassa*. *Curr Opin Microbiol* 10: 199–203.
77. Shiu PKT, Raju NB, Zickler D, Metzberg RL (2001) Meiotic silencing by unpaired DNA. *Cell* 107: 905–916.
78. Engh I, Nowrousian M, Kück U (2007) Regulation of melanin biosynthesis via the dihydroxynaphthalene pathway is dependent on sexual development in the ascomycete *Sordaria macrospora*. *FEMS Microbiol Lett* 275: 62–70.
79. Nowrousian M, Piotrowski M, Kück U (2007) Multiple layers of temporal and spatial control regulate accumulation of the fruiting body-specific protein APP in *Sordaria macrospora* and *Neurospora crassa*. *Fungal Genet Biol* 44: 602–614.
80. Kück U (2005) A *Sordaria macrospora* mutant lacking the *leu1* gene shows a developmental arrest during fruiting body formation. *Mol Genet Genomics* 274: 307–315.
81. Borkovich KA, Alex LA, Yarden O, Freitag M, Turner GE, et al. (2004) Lessons from the genome sequence of *Neurospora crassa*: tracing the path from genomic blueprint to multicellular organism. *Microbiol Mol Biol Rev* 68: 1–108.
82. Zickler D (2009) Observing meiosis in filamentous fungi: *Sordaria* and *Neurospora*. *Methods Mol Biol* 558: 91–114.
83. Nowrousian M, Kück U (2006) Comparative gene expression analysis of fruiting body development in two filamentous fungi. *FEMS Microbiol Lett* 257: 328–335.
84. Harding RW, Melles S (1983) Genetic analysis of phototropism of *Neurospora crassa* perithecial beaks using white collar and albino mutants. *Plant Physiol* 72: 996–1000.
85. Read ND (1983) A scanning electron microscopic study of the external features of perithecium development in *Sordaria humana*. *Can J Bot* 61: 3217–3229.
86. Froehlich AC, Liu Y, Loros JJ, Dunlap JC (2002) White Collar-1, a circadian blue light photoreceptor, binding to the *frequency* promoter. *Science* 297: 815–819.
87. He Q, Cheng P, Yang Y, Wang L, Gardner K, et al. (2002) White collar-1, a DNA binding transcription factor and a light sensor. *Science* 297: 840–843.
88. Ballario P, Vittorioso P, Magrelli A, Talora C, Cabibbo A, et al. (1996) White collar-1, a central regulator of blue-light responses in *Neurospora*, is a zinc finger protein. *EMBO J* 15: 1650–1657.
89. Purschitz J, Müller S, Kastner C, Schöser M, Haas H, et al. (2008) Functional and physical interaction of blue- and red-light sensors in *Aspergillus nidulans*. *Curr Biol* 18: 255–259.
90. Blumenstein A, Vienken K, Tasler R, Purschwitz J, Veith D, et al. (2005) The *Aspergillus nidulans* phytochrome FphA represses sexual development in red light. *Current Biology* 15: 1833–1838.
91. Linden H, Ballario P, Arpaia G, Macino G (1999) Seeing the light: News in *Neurospora* blue light signal transduction. *Adv Genet* 41: 35–54.
92. Bieszke JA, Spudich EN, Scott KL, Borkovich KA, Spudich JL (1999) A eukaryotic protein, NOP-1, binds retinal to form an archaeal rhodopsin-like photochemically reactive pigment. *Biochemistry* 38: 14138–14145.
93. Griffiths AJ (1992) Fungal senescence. *Annu Rev Genet* 26: 351–372.
94. Osiewacz HD (1990) Molecular analysis of aging processes in fungi. *Mut Res* 237: 1–8.
95. Wu M, Xu L-G, Li X, Zhai Z, Shu H-B (2002) AMID, an apoptosis-inducing factor-homologous mitochondrion-associated protein, induces caspase-independent apoptosis. *J Biol Chem* 277: 25617–25623.
96. Averbach NB, Jensen ON, Mann M, Schagger H, Osiewacz HD (2000) Identification and characterization of PaMTH1, a putative O-methyltransferase accumulating during senescence of *Podospora anserina* cultures. *Curr Genet* 37: 200–208.
97. Groche K, Krause F, Kunstmann B, Unterlugauer H, Reifschneider NH, et al. (2007) Differential proteomic profiling of mitochondria from *Podospora anserina*, rat and human reveals distinct patterns of age-related oxidative changes. *Exp Gerontol* 42: 887–898.
98. Kunstmann B, Osiewacz HD (2008) Over-expression of an S-adenosylmethionine-dependent methyltransferase leads to an extended lifespan of *Podospora anserina* without impairments in vital functions. *Aging Cell* 7: 651–662.
99. Kunstmann B, Osiewacz HD (2009) The S-adenosylmethionine dependent O-methyltransferase PaMTH1: a longevity assurance factor protecting *Podospora anserina* against oxidative stress. *Aging* 1: 328–334.
100. Mata J, Lyne R, Burns G, Bähle rj (2002) The transcriptional program of meiosis and sporulation in fission yeast. *Nat Genet* 32: 143–147.
101. Schlecht U, Primig M (2003) Mining meiosis and gametogenesis with DNA microarrays. *Reproduction* 225: 447–456.
102. Espagne E, Lespinet O, Malagnac F, Da Silva C, Jaillon O, et al. (2008) The genome sequence of the model ascomycete fungus *Podospora anserina*. *Genome Biol* 9: R77.
103. Page SL, Hawley RS (2004) The genetics and molecular biology of the synaptonemal complex. *Annu Rev Cell Dev Biol* 20: 525–558.
104. Malik SB, Pightling AW, Stefaniak LM, Schurko AM, Logsdon JM (2008) An expanded inventory of conserved meiotic genes provides evidence for sex in *Trichomonas vaginalis*. *PLOS ONE* 3: e2879. doi:10.1371/journal.pone.0002879.
105. Hunter N (2006) Meiotic recombination. In: Aguilera A, Rothstein R, eds. *Molecular genetics of recombination*. Berlin, Heidelberg: Springer. pp 381–443.
106. O'Gorman CM, Fuller HT, Dyer PS (2009) Discovery of a sexual cycle in the opportunistic fungal pathogen *Aspergillus fumigatus*. *Nature* 457: 471–475.
107. Pöggeler S (2002) Genomic evidence for mating abilities in the asexual pathogen *Aspergillus fumigatus*. *Curr Genet* 42: 153–160.
108. Read ND, Fleissner A, Roca MG, Glass NL (2010) Hyphal fusion. In: Borkovich KA, Ebbole D, eds. *Molecular biology of filamentous fungi* Am. Soc. Microbiol. pp 260–273.
109. Saupe S (2000) Molecular genetics of heterokaryon incompatibility in filamentous ascomycetes. *Microbiol Mol Biol Rev* 64: 489–502.
110. Micali OC, Smith ML (2006) A nonself recognition gene complex in *Neurospora crassa*. *Genetics* 173: 1991–2004.
111. Cortesi P, McCulloch CE, Song H, Lin H, Milgroom MG (2001) Genetic control of horizontal virus transmission in the chestnut blight fungus, *Cryphonectria parasitica*. *Genetics* 159: 107–118.
112. Debets A, Griffiths AJ (1998) Poyomorphism of het genes prevents resource plundering in *Neurospora crassa*. *Mycol Res* 102: 1343–1349.
113. Debets F, Yang X, Griffiths AJ (1994) Vegetative incompatibility in *Neurospora*: its effect on horizontal transfer of mitochondrial plasmids and senescence in natural populations. *Curr Genet* 26: 113–119.
114. van Diepeningen AD, Debets AJ, Hockstra RF (1997) Heterokaryon incompatibility blocks virus transfer among natural isolates of black Aspergilli. *Curr Genet* 32: 209–217.

115. Glass NL, Kaneko I (2003) Fatal attraction: nonself recognition and heterokaryon incompatibility in filamentous fungi. *Eukaryot Cell* 2: 1–8.
116. Smith ML, Micali OC, Hubbard SP, Mir-Rashed N, Jacobson DJ, et al. (2000) Vegetative incompatibility in the het-6 region of *Neurospora crassa* is mediated by two linked genes. *Genetics* 155: 1095–1104.
117. Paoletti M, Saupe SJ, Clavé C (2007) Genesis of a fungal non-self recognition repertoire. *PLoS ONE* 2: e283. doi:10.1371/journal.pone.0000283.
118. Beadle GW, Conradt VL (1944) Heterocaryosis in *Neurospora crassa*. *Genetics* 29: 291–308.
119. Espagne E, Balhadère P, Penin ML, Barreau C, Turcq B (2002) HET-E and HET-D belong to a new subfamily of WD40 proteins involved in vegetative incompatibility specificity in the fungus *Podospora anserina*. *Genetics* 161: 71–81.
120. Shiu PK, Glass NL (1999) Molecular characterization of tol, a mediator of mating-type-associated vegetative incompatibility in *Neurospora crassa*. *Genetics* 151: 545–555.
121. Fedorova N, Badger J, Robson G, Wortman J, Niernan W (2005) Comparative analysis of programmed cell death pathways in filamentous fungi. *BMC Genomics* 6: 177.
122. Kaneko I, Dementhon K, Xiang Q, Glass NL (2006) Nonallelic interactions between het-c and a polymorphic locus, pin-c, are essential for nonself recognition and programmed cell death in *Neurospora crassa*. *Genetics* 172: 1545–1555.
123. Sarkar S, Iyer G, Wu J, Glass NL (2002) Nonself recognition is mediated by HET-C heterocomplex formation during vegetative incompatibility. *EMBO J* 21: 4841–4850.
124. Jacobson DJ, Beurkens K, Klomarens KL (1998) Microscopic and ultrastructural examination of vegetative incompatibility in partial diploids heterozygous at *het loci* in *Neurospora crassa*. *Fungal Genet Biol* 23: 45–56.
125. Mylek OM (1975) Heterokaryon incompatibility genes in *Neurospora crassa* detected using duplication-producing chromosome rearrangements. *Genetics* 80: 107–124.
126. Perkins DD (1975) The use of duplication-generating rearrangements for studying heterokaryon incompatibility genes in *Neurospora*. *Genetics* 80: 87–105.
127. Wu J, Glass NL (2001) Identification of specificity determinants and generation of alleles with novel specificity at the het-c heterokaryon incompatibility locus of *Neurospora crassa*. *Mol Cell Biol* 21: 1045–1057.
128. Pöggeler S, Risch S, Kück U, Osiewacz HD (1997) Mating-type genes from the homothallic fungus *Sordaria macrospora* are functionally expressed in a heterothallic ascomycete. *Genetics* 147: 567–580.
129. Jacobson DJ (1992) Control of mating type heterokaryon incompatibility by the *tol* gene in *Neurospora crassa* and *N. tetrasperma*. *Genome* 35: 347–353.
130. Mir-Rashed N, Jacobson DJ, Dehghany MR, Micali OC, Smith ML (2000) Molecular and functional analyses of incompatibility genes at *het-6* in a population of *Neurospora crassa*. *Fungal Genet Biol* 30: 197–205.
131. Powell AJ, Jacobson DJ, Natvig DO (2007) Ancestral polymorphism and linkage disequilibrium at the *het-6* region in pseudohomothallic *Neurospora tetrasperma*. *Fungal Genet Biol* 44: 896–904.
132. Cox RJ (2007) Polyketides, proteins and genes in fungi: programmed nanomachines begin to reveal their secrets. *Org Biomol Chem* 5: 2010–2026.
133. Walsh CT (2004) Polyketide and nonribosomal peptide antibiotics: modularity and versatility. *Science* 303: 1805–1810.
134. Keller NP, Hohn TM (1997) Metabolic pathway gene clusters in filamentous fungi. *Fungal Genet Biol* 21: 17–29.
135. Kroken S, Glass NL, Taylor JW, Yoder OC, Turgeon BG (2003) Phylogenomic analysis of type I polyketide synthase genes in pathogenic and saprobic ascomycetes. *Proc Natl Acad Sci USA* 100: 15670–15675.
136. Hane JK, Lowe RGT, Solomon PS, Tan K-C, Schoch CL, et al. (2007) Dothideomycete plant interactions illuminated by genome sequencing and EST analysis of the wheat pathogen *Stagonospora nodorum*. *Plant Cell* 19: 3347–3368.
137. Rosewich UL, Kistler HC (2000) Role of horizontal gene transfer in the evolution of fungi. *Annu Rev Phytopathol* 38: 326–363.
138. Khaldi N, Wolfe KH (2008) Elusive origins of the extra genes in *Aspergillus oryzae*. *PLoS ONE* 3: e3036. doi:10.1371/journal.pone.0003036.
139. Patron NJ, Waller RF, Cozijnsen AJ, Straney DC, Gardiner DM, et al. (2007) Origin and distribution of epipolythiodioxopiperazine (ETP) gene clusters in filamentous ascomycetes. *BMC Evol Biol* 7: 174.
140. Khaldi N, Collemare J, Lebrun M-H, Wolfe KH (2008) Evidence for horizontal transfer of a secondary metabolite gene cluster between fungi. *Genome Biol* 9: R18.
141. Friesen TL, Stukenbrock EH, Liu Z, Meinhardt S, Ling H, et al. (2006) Emergence of a new disease as a result of interspecific virulence gene transfer. *Nat Genet* 38: 953–956.
142. Fedorova ND, Khaldi N, Joardar VS, Maiti R, Amedeo P, et al. (2008) Genomic islands in the pathogenic filamentous fungus *Aspergillus fumigatus*. *PLoS Genet* 4: e1000046. doi:10.1371/journal.pgen.1000046.
143. Garcia-Vallvé S, Romeu A, Palau J (2000) Horizontal gene transfer of glycosyl hydrolases of the rumen fungi. *Mol Biol Evol* 17: 352–361.
144. Coleman JJ, Rounsley SD, Rodriguez-Carres M, Kuo A, Wasmann CC, et al. (2009) The genome of *Nectria haematococca*: Contribution of supernumerary chromosomes to gene expansion. *PLoS Genet* 5: e1000618. doi:10.1371/journal.pgen.1000618.
145. Hoge JHC, Springer J, Zantinge B, Wessels JGH (1982) Absence of differences in polysomal RNAs from vegetative monokaryotic and dikaryotic cells of the fungus *Schizophyllum commune*. *Exp Mycol* 6: 225–232.
146. Pomraning KR, Smith KM, Freitag M (2009) Genome-wide high throughput analysis of DNA methylation in eukaryotes. *Methods* 47: 142–150.
147. Altschul SF, Madden TL, Schaffer AA, Zhang J, Zhang Z, et al. (1997) Gapped BLAST and PSI-BLAST: a new generation of protein database search programs. *Nucleic Acids Res* 25: 3389–3402.
148. Engels R, Yu T, Burge C, Mesirov JP, DeCaprio D, et al. (2006) Combo: a whole genome comparative browser. *Bioinformatics* 22: 1782–1783.
149. Korf I (2004) Gene finding in novel genomes. *BMC Bioinformatics* 5: 59.
150. Stanke M, Schöffmann O, Morgenstern B, Waack S (2006) Gene prediction in eukaryotes with a generalized hidden Markov model that uses hints from external sources. *BMC Bioinformatics* 7: 62.
151. Stanke M, Waack S (2003) Gene prediction with a hidden Markov model and a new intron submodel. *Bioinformatics* 19(suppl. 2): ii215–225.
152. Besemer J, Borodovsky M (2005) GeneMark: web software for gene finding in prokaryotes, eukaryotes and viruses. *Nucl Acids Res* 33: W451–454.
153. Birney E, Clamp M, Durbin R (2004) GeneWise and Genomewise. *Genome Res* 14: 988–955.
154. Stajich JE, Block D, Boulez K, Brenner SE, Chervitz SA, et al. (2002) The Bioperl Toolkit: Perl modules for the life sciences. *Genome Res* 12: 1611–1618.
155. Horton P, Park KJ, Obayashi T, Nakai K (2006) Protein subcellular localization prediction with WoLF PSORT. *Proceedings of the 4th Annual Asia Pacific Bioinformatics Conference APBC06*, Taipei, Taiwan. pp 39–48.
156. Bendtsen JD, Nielsen H, von Heijne G, Brunak S (2004) Improved prediction of signal peptides: SignalP 3.0. *J Mol Biol* 340: 783–795.
157. Tusnady GE, Simon I (1998) Principles governing amino acid composition of integral membrane proteins: Applications to topology prediction. *J Mol Biol* 283: 489–506.
158. Krogh A, Larsson B, von Heijne G, Sonnhammer ELL (2001) Predicting transmembrane protein topology with a hidden Markov model: Application to complete genomes. *J Mol Biol* 305: 567–580.
159. Lowe TM, Eddy SR (1997) tRNAscan-SE: a program for improved detection of transfer RNA genes in genomic sequence. *Nucl Acids Res* 25: 955–964.
160. Nawrocki EP, Kolbe DL, Eddy SR (2009) Infernal 1.0: inference of RNA alignments. *Bioinformatics* 25: 1335–1337.
161. Taqut H, Cui Y, Ardell DH (2007) tFAM 1.0: an online tRNA function classifier. *Nucl Acids Res* 35: W350–353.
162. Nowrousian M, Cebula P (2005) The gene for a lectin-like protein is transcriptionally activated during sexual development, but is not essential for fruiting body formation in the filamentous fungus *Sordaria macrospora*. *BMC Microbiol* 5: 64.
163. Thompson JD, Gibson TJ, Plewniak F, Jeanmougin F, Higgins DG (1997) The ClustalX windows interface: flexible strategies for multiple sequence alignment aided by quality analysis tools. *Nucleic Acids Res* 24: 4876–4882.
164. Waterhouse AM, Procter JB, Martin DMA, Clamp M, Barton GJ (2009) Jalview Version 2 - a multiple sequence alignment editor and analysis workbench. *Bioinformatics* 25: 1189–1191.
165. Huelsenbeck JP, Ronquist F (2001) Bayesian inference of phylogeny. *Bioinformatics* 17: 754–755.
166. Ronquist F, Huelsenbeck JP (2003) Bayesian phylogenetic inference under mixed models. *Bioinformatics* 19: 1572–1574.
167. Hall BG (2004) Phylogenetic trees made easy. Sunderland: Sinauer Associates.
168. Huson DH, Richter DC, Rausch C, Dezulian T, Franz M, et al. (2007) Dendroscope - An interactive viewer for large phylogenetic trees. *BMC Bioinformatics* 8: 460.
169. Page R (1996) TREEVIEW: an application to display phylogenetic trees on personal computers. *Appl Biosci* 12: 357–358.
170. Dementhon K, Iyer G, Glass NL (2006) VIB-1 Is required for expression of genes necessary for programmed cell death in *Neurospora crassa*. *Eukaryot Cell* 5: 2161–2173.
171. Liu YJ, Hall BD (2004) Body plan evolution of ascomycetes, as inferred from an RNA polymerase II phylogeny. *Proc Natl Acad Sci USA* 101: 4507–4512.